# *Shear enhanced decompaction weakening and its effects on formation of seismic chimney*

Lawrence Hongliang Wang  Viktoriya Yarushina, Yury Podladchikov

**Department of Environmental Analyses, Institute of Energy Technology, Norway**

**University of Lausanne, Institute of Earth Sciences, Lausanne, Switzerland**

CO2 Path project: Prediction of CO2 leakage from reservoirs during large scale storage

The Research Council of Norway

# Seismic chimneys from observations

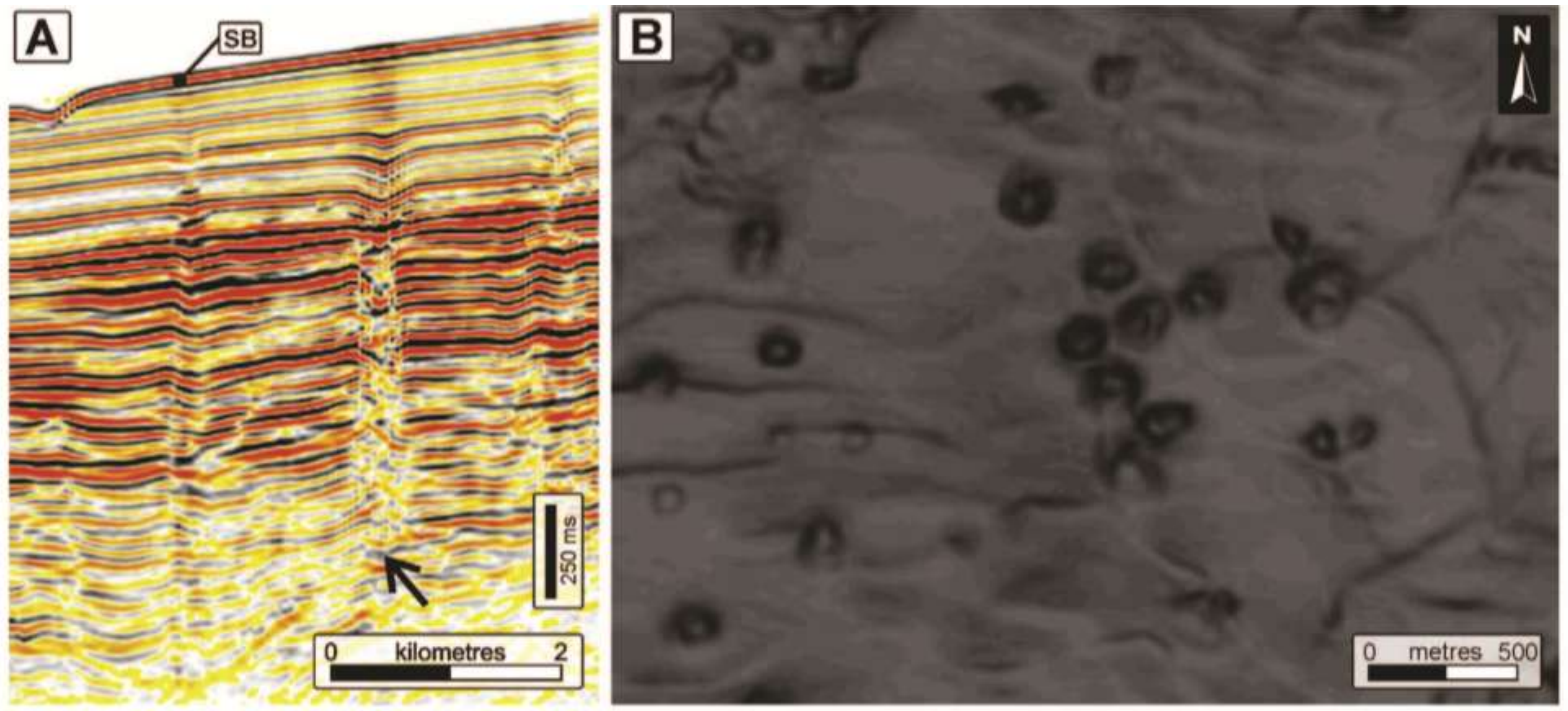


Cartwright and Santamarina, 2015

Offshore Namibia

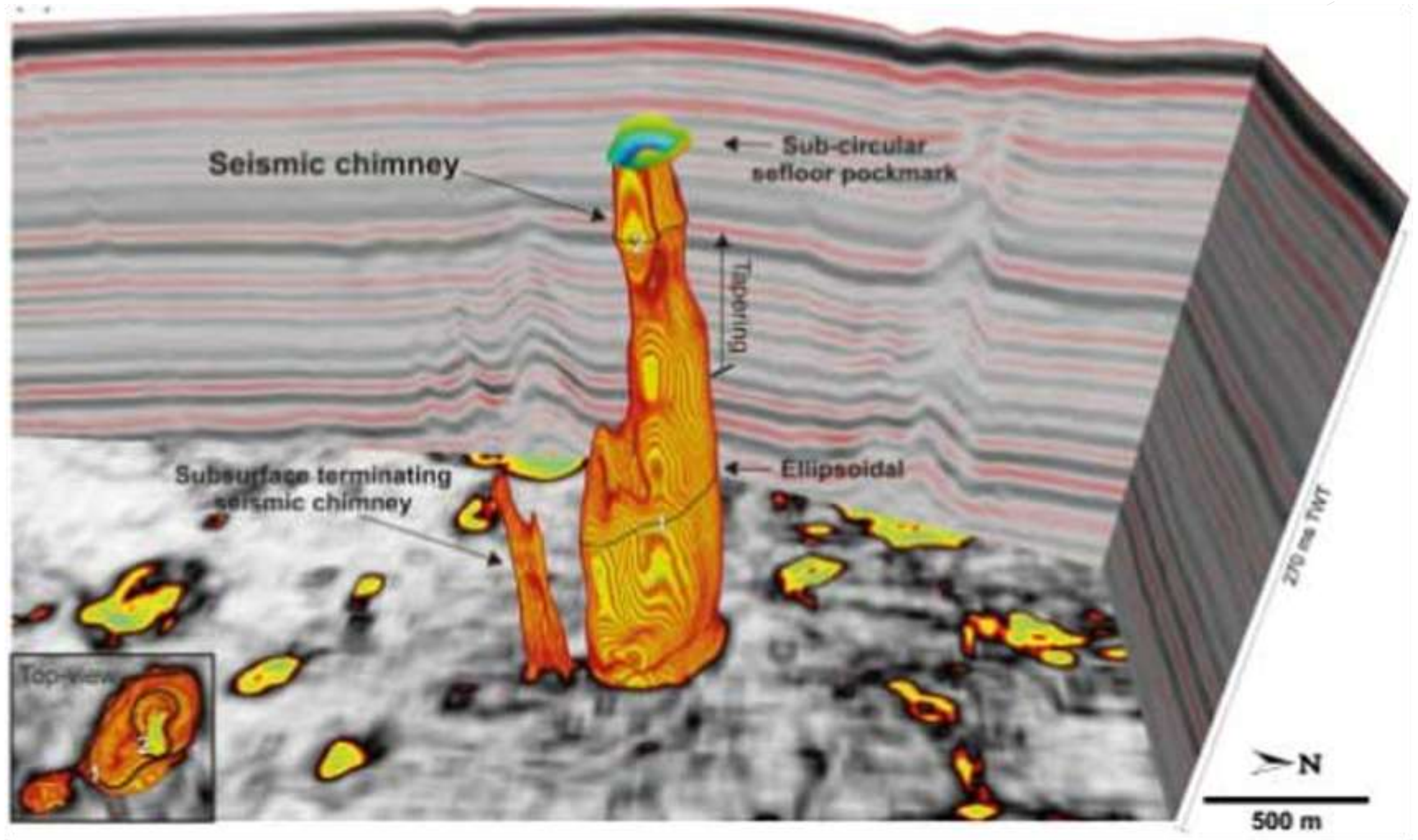


Nyegga area, mid-Norwegian continental margin

- Seismic chimeys and pockmark field
- Focalized fluid flow

- Cross section From nearly circular to elliptical
- Long axis from ~100 m to 900 m

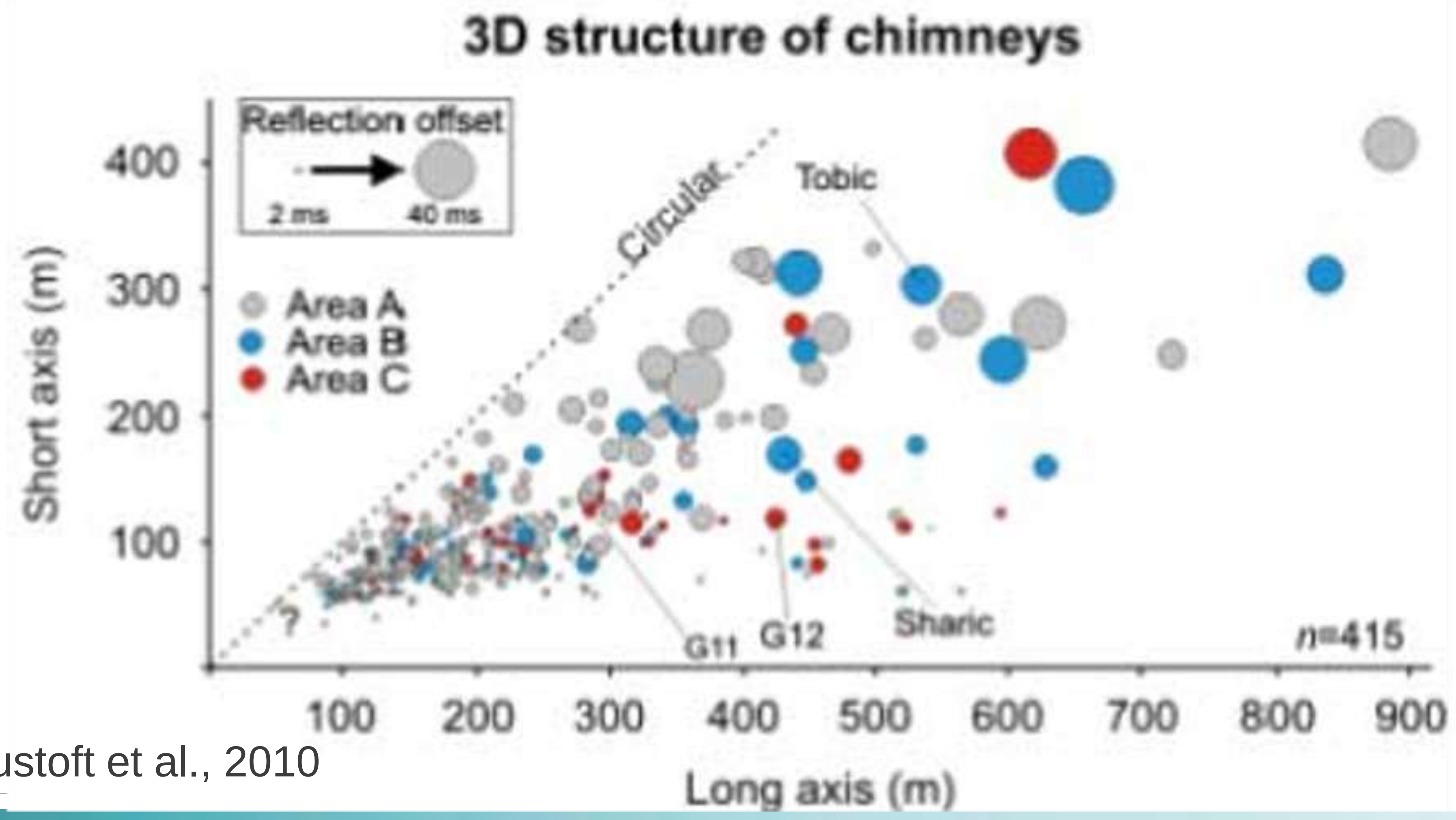


Hustoft et al., 2010

# $CO_2$ plumes at Sleipner

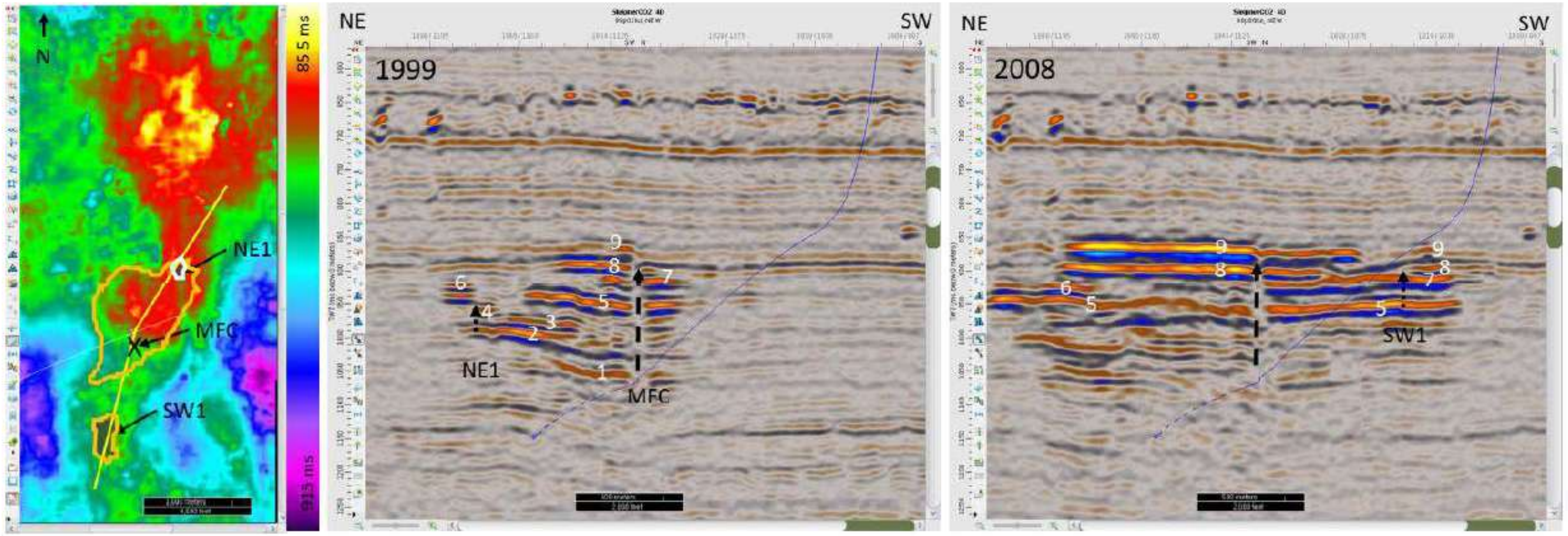


Furre, et al., 2019

~250 m nordland GP shale as the seal

26 m Pliocene sand wedge

6m shale layer

Utsira formation (reservior)

Seismic observation shows that arising plume of $CO_2$ flow forms within the reservoir and spread out underneath the caprock. Would it cause $CO_2$ leakage in the future? What is the mechanism and how to avoid it ?

# Potential Mechanisms

- 1. **Hydralic fracture: i.e brittle rock**
- 2. erosive fluidization
- 3. Capillary invasion

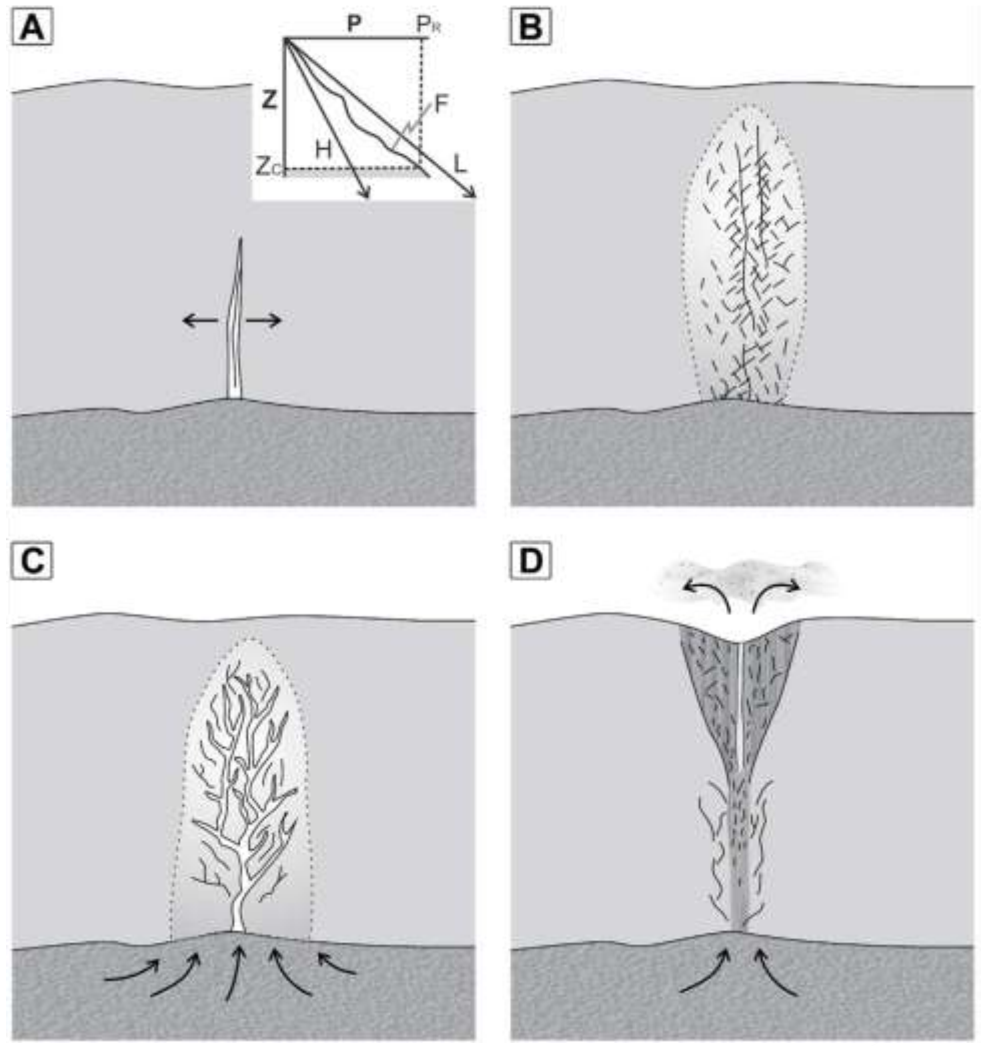


Cartwright and Santamarina, 2015

4. **Porous waves with decompaction weakening:**
Two-phase flow theory: solid + fluid
Fluid migration through opening (decompaction) and closing (compaction) poro-space in the solid matrix

asymmetric bulk viscosity for compaction and decompaction

Decompaction

Compaction

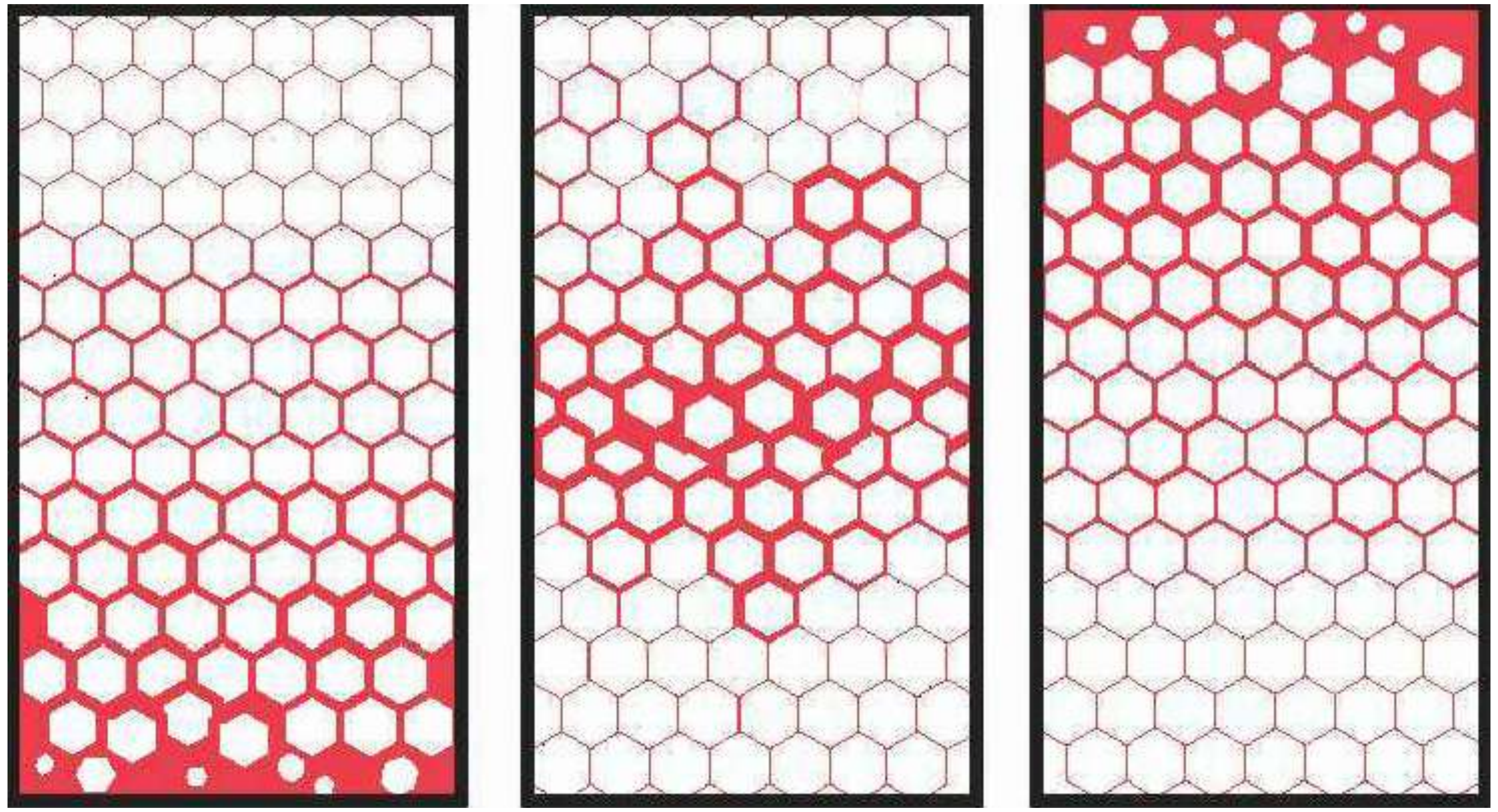

Richard & Schmeling. 2008

# Governing equations and numerical methods

Mass balance

$$\frac{\partial \rho_s(1-\varphi)}{\partial t} + \nabla(\rho_s(1-\varphi)v_s) = 0$$

$$\frac{\partial \rho_f \varphi}{\partial t} + \nabla(\rho_f \varphi v_f) = 0$$

Force balance

$$\frac{\partial \sigma_{ij}^{eff}}{\partial x_j} - \frac{\partial p_f}{\partial x_i} = g\bar{\rho}\hat{z}$$

Darcy flow

$$\varphi(v_f - v_s) = -\frac{k(\varphi)}{\mu_f}\nabla\left(p_f + \rho_f g z\right)$$

Permeability $k = \mathrm{k0}\,(\frac{\phi}{\phi_0})^3$

Bulk viscosity $\eta_\phi = \mathrm{f}(\mathrm{Pe}, \phi, \tau)$ ?

Yarushina & Podladchikov. 2015

**Pseudo-Transient method**

add Pseudo time-derivative at right side

$$\nabla_k \boldsymbol{v_k}^s + \frac{P_e}{\eta_\phi(1-\phi)} = 0 \qquad = \frac{dP}{d\tau_p}$$

$$\nabla_j(\tau_{ij} - P\delta_{ij}) - \bar{\rho} g_i = 0 \qquad = \frac{dv_i{}^s}{d\tau_v}$$

$$\nabla_k(\boldsymbol{v_k}^f - \boldsymbol{v_k}^s)\phi - \frac{P_e}{\eta_\phi(1-\phi)} = 0 \qquad = \frac{dP^f}{d\tau_p{}^f}$$

Local physics

No matrix

Less memory

Numerical dampening: use the physics of the damped wave propagation to speed up the iteration.

Err= $\mathrm{A}\ \mathrm{e}^{-\lambda t}\mathrm{e}^{kx}$

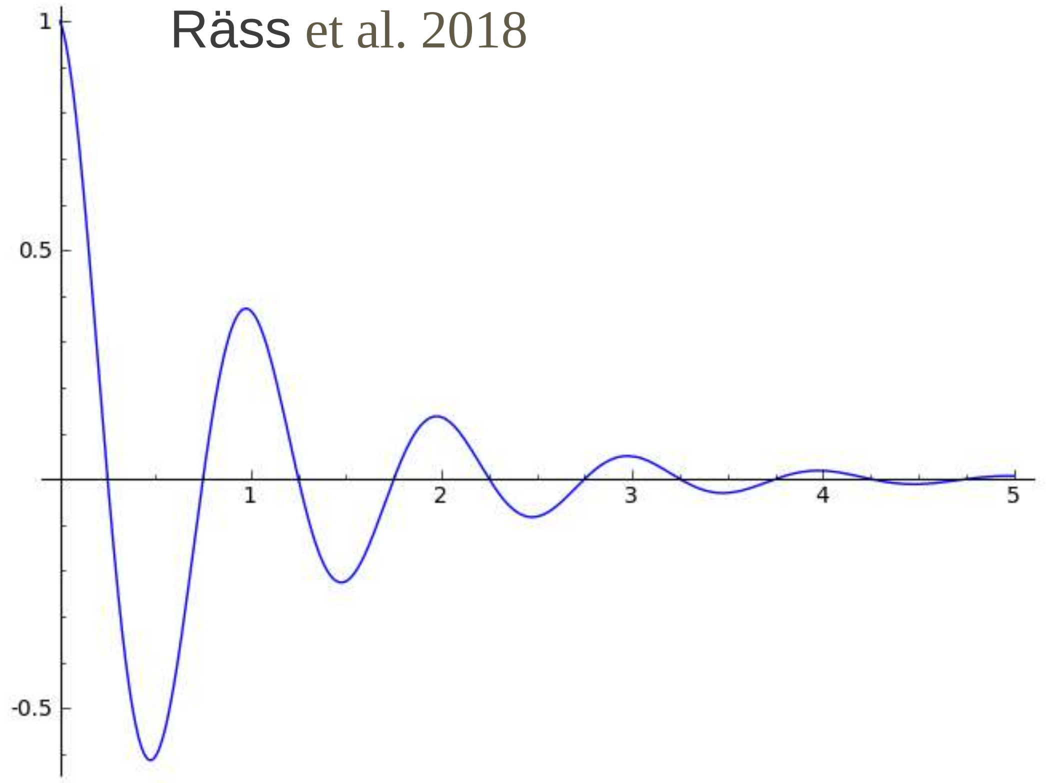


Räss et al. 2018

# Bulk Viscosity：Type 1 and 2

## Type 1

$$\eta_{eff} = \eta_{\phi}(1+\frac{1}{2}(\frac{1}{R}-1)(1+\tanh(-\frac{Pe}{\lambda_p}))$$

Bulk viscosity is R times smaller, when effective pressure ($P_e = P_f - P_t$) is positive (decompaction).

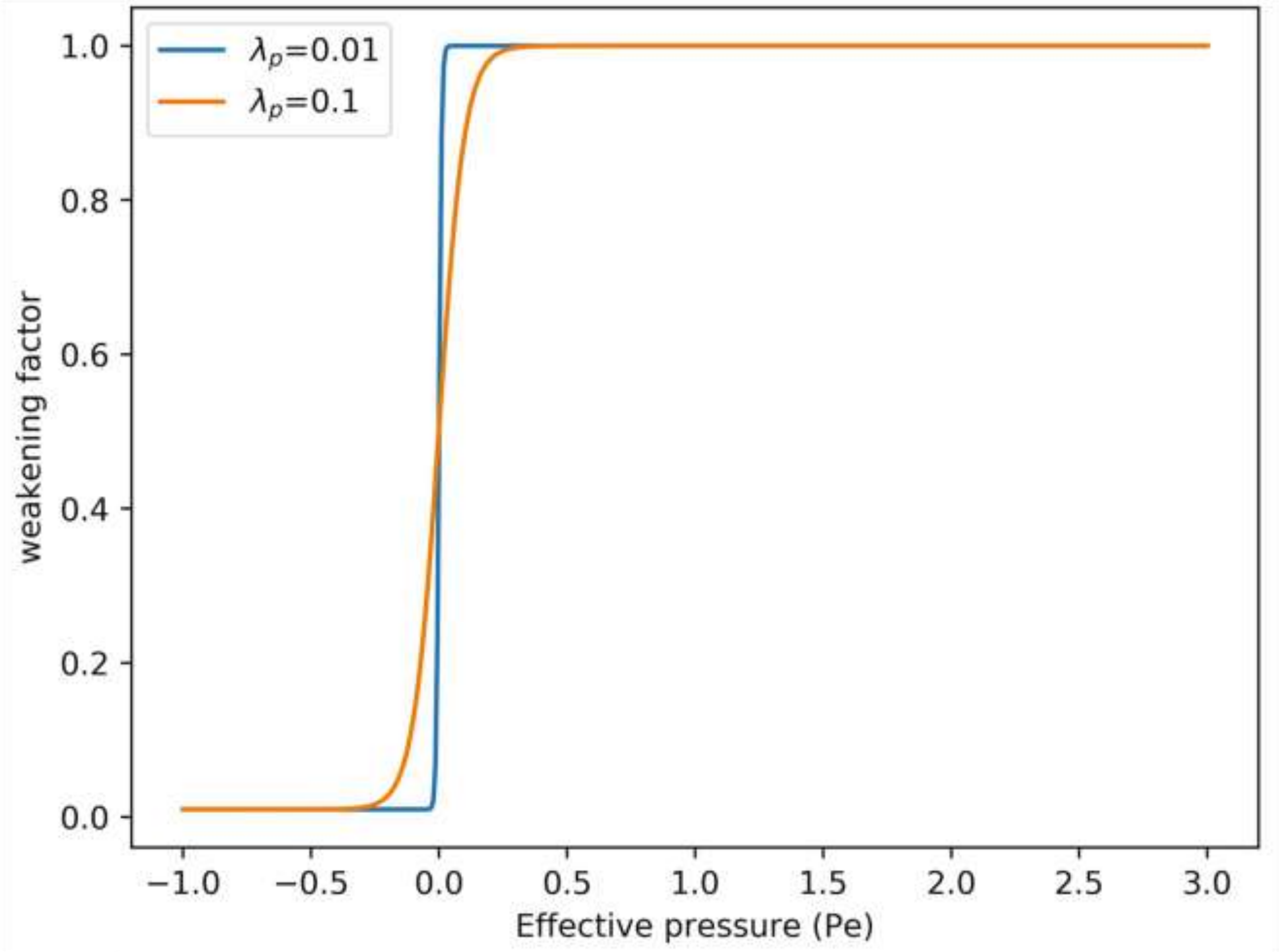


Räss et al. 2018

## Type 2

$$\eta_{eff} = \eta_{\varphi}\begin{cases} 1, & -k_d < P_e < k_c \\ \frac{|P_e|}{k_e}\exp\left(1-\frac{|P_e|}{k_e}\right) & \end{cases} \quad k_e = \begin{cases} k_c, when\ P_e > 0 \\ k_d, when\ P_e < 0 \end{cases}$$

Different compressive strength ($k_c$) and tensile strength ($k_d$), from experiment data.

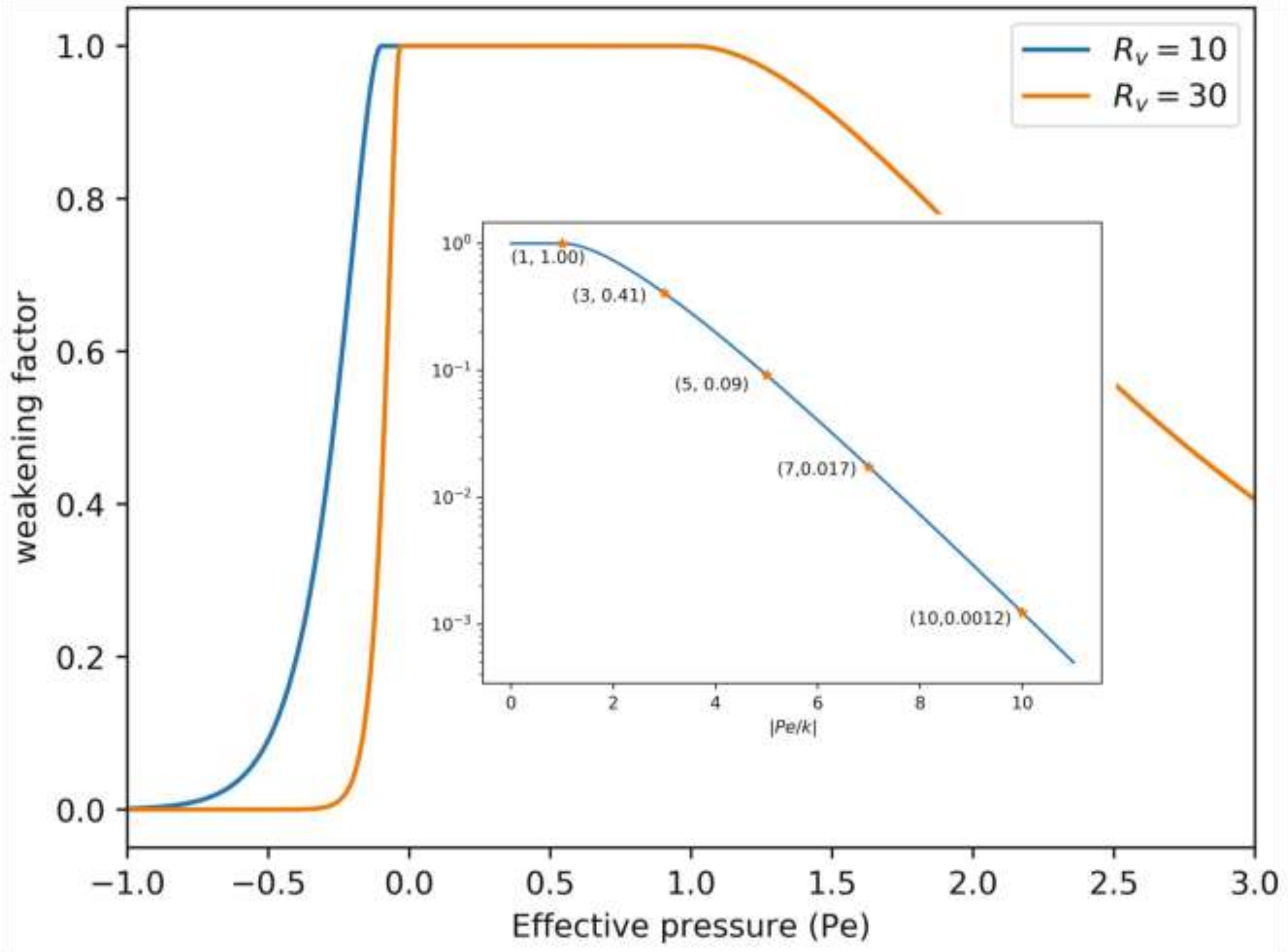


Yarushina et al. 2019 (in preparation)

# Bulk Viscosity : Type 3 = Type 2 + shear enhancement

## Type 3

Further weakening by shear stress

$$\eta_{eff} = \eta_{\varphi} \begin{cases} 1\,, \\ \dfrac{|P_e|}{k_e} \exp\left(1 - \dfrac{|P_e|}{k_e}\right)\left(1 + \left(\dfrac{\tau}{\tau_e}\right)^n\right)^{-1} \end{cases}$$

$$F = \left(1 + \left(\frac{\tau}{\tau_c}\right)^n\right) \exp\left(\frac{P_e}{k_c} - 1\right) k_c - k_c > 0$$

$$F = \left(1 + \left(\frac{\tau}{\tau_c}\right)^n\right) \exp\left(\frac{P_e}{k_d} + 1\right) k_d - k_d > 0$$

$$\tau_e = \begin{cases} \tau_c, when\ \mathrm{P}_e > 0 \\ \tau_d, when\ \mathrm{P}_e < 0 \end{cases} \qquad \mathrm{k}_e = \begin{cases} \mathrm{k}_c, when\ \mathrm{P}_e > 0 \\ \mathrm{k}_d, when\ \mathrm{P}_e < 0 \end{cases}$$

Yarushina et al. 2019 (in preparation)

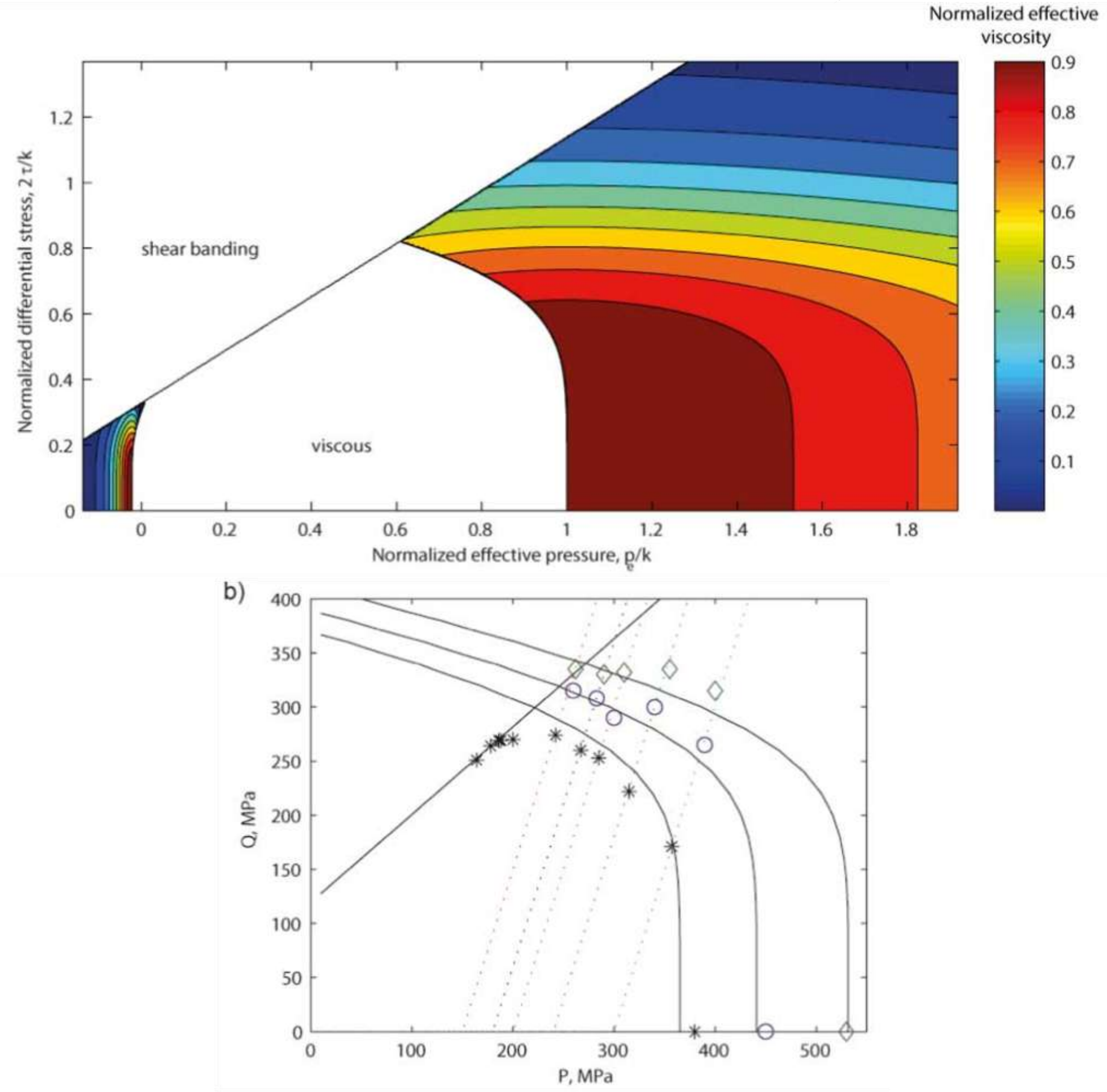

# Reference model

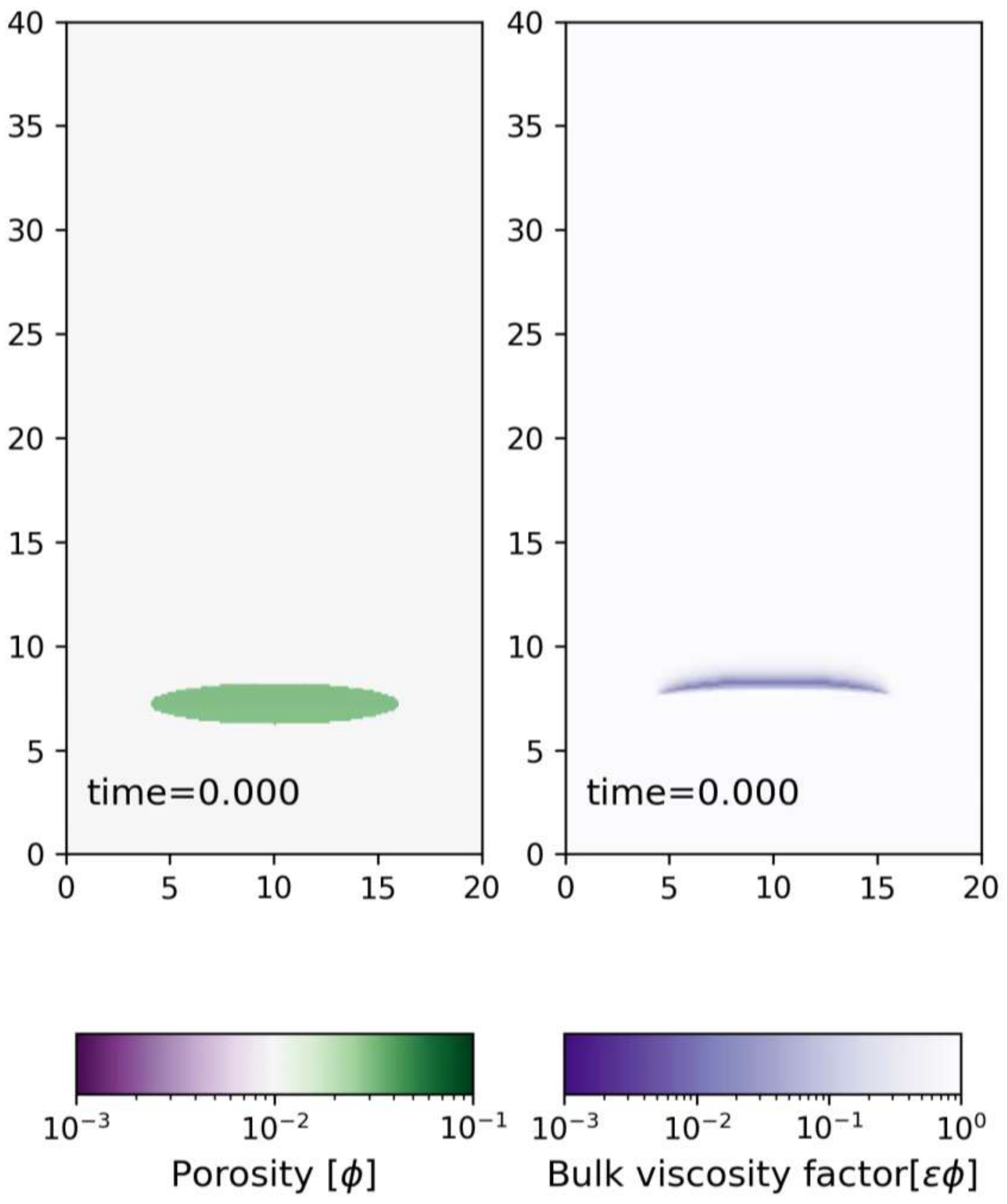

# Result: Type 1 (R=10,100,1000)

## R= 10

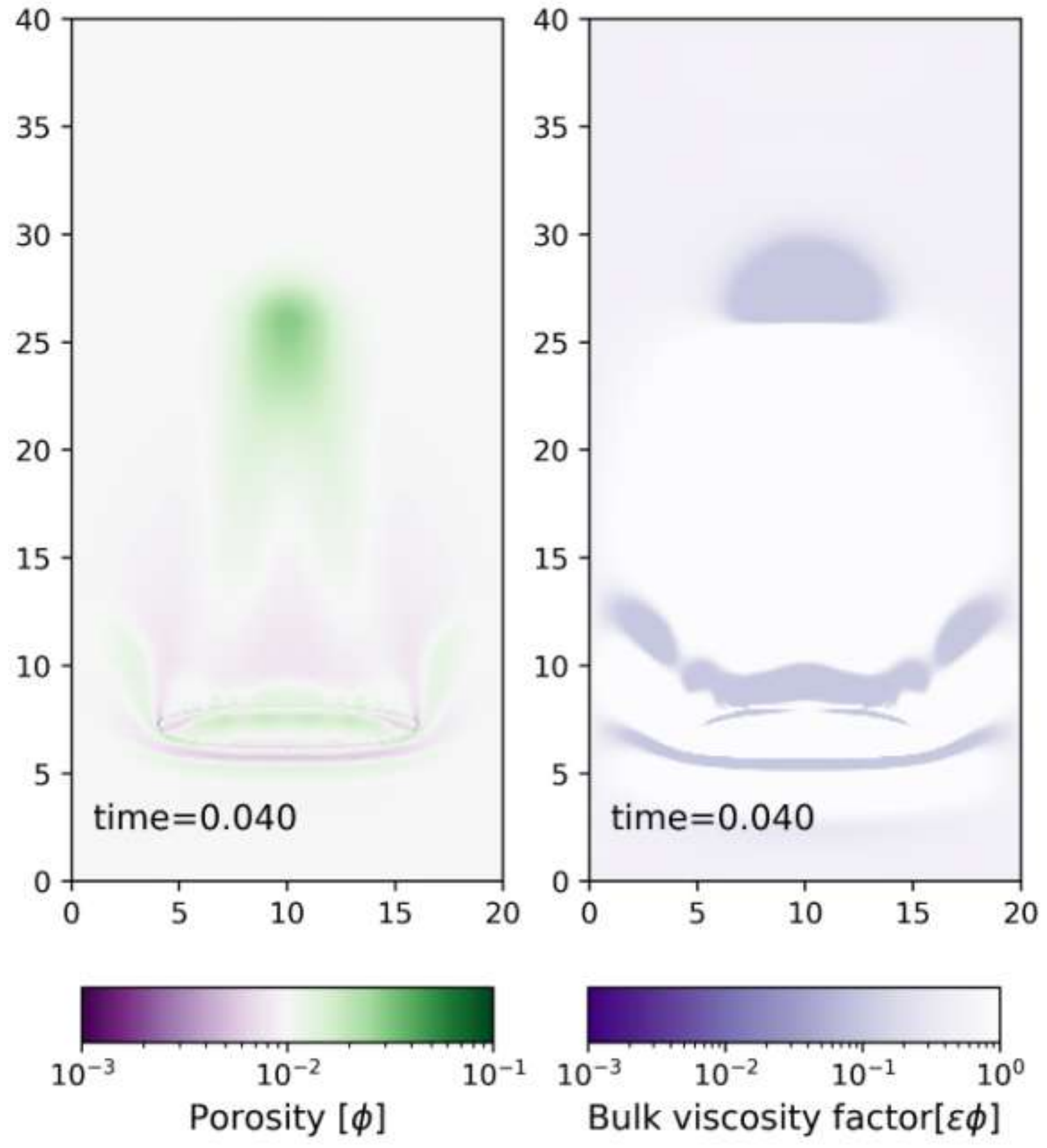


## R= 100

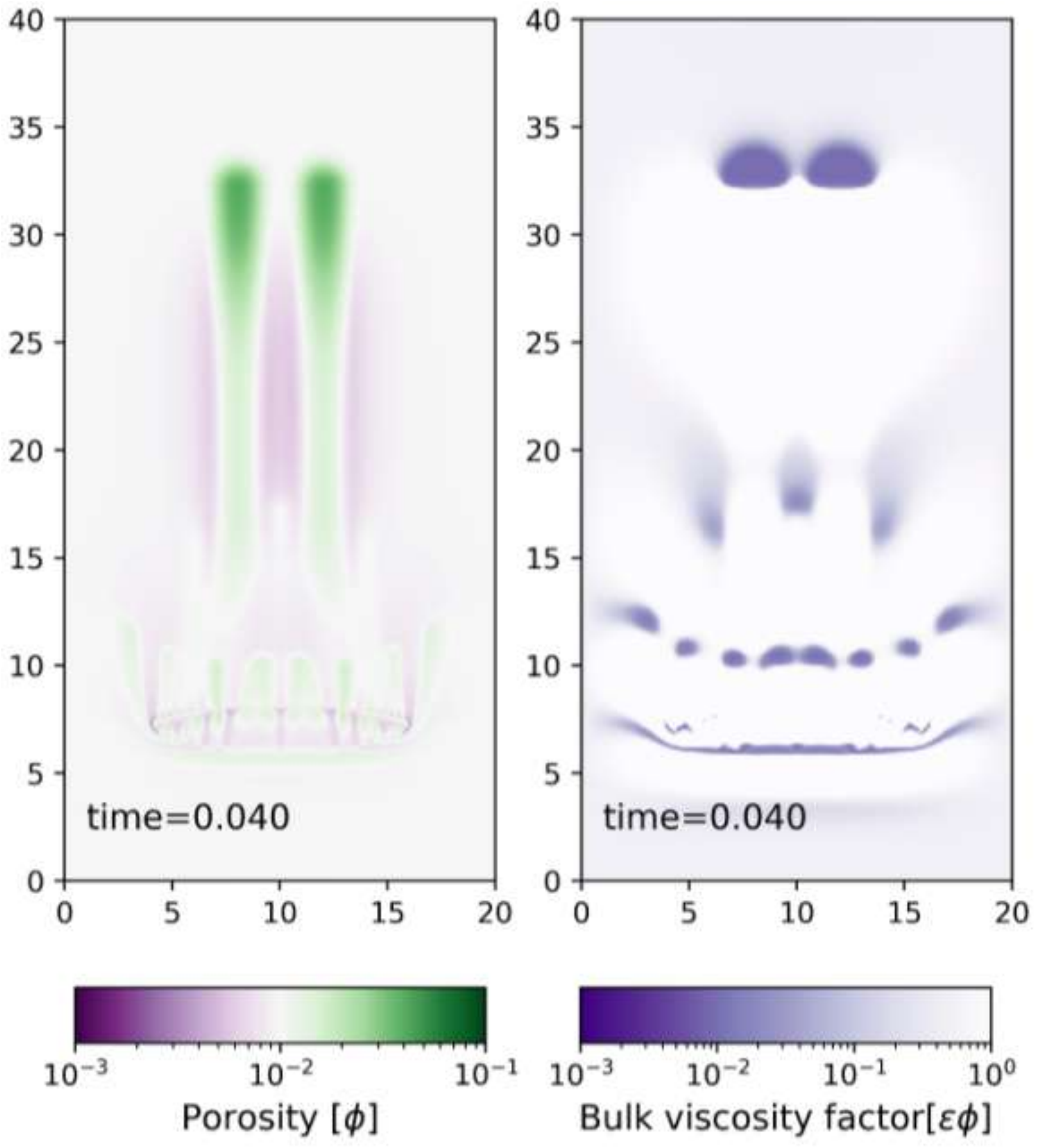


## R= 1000

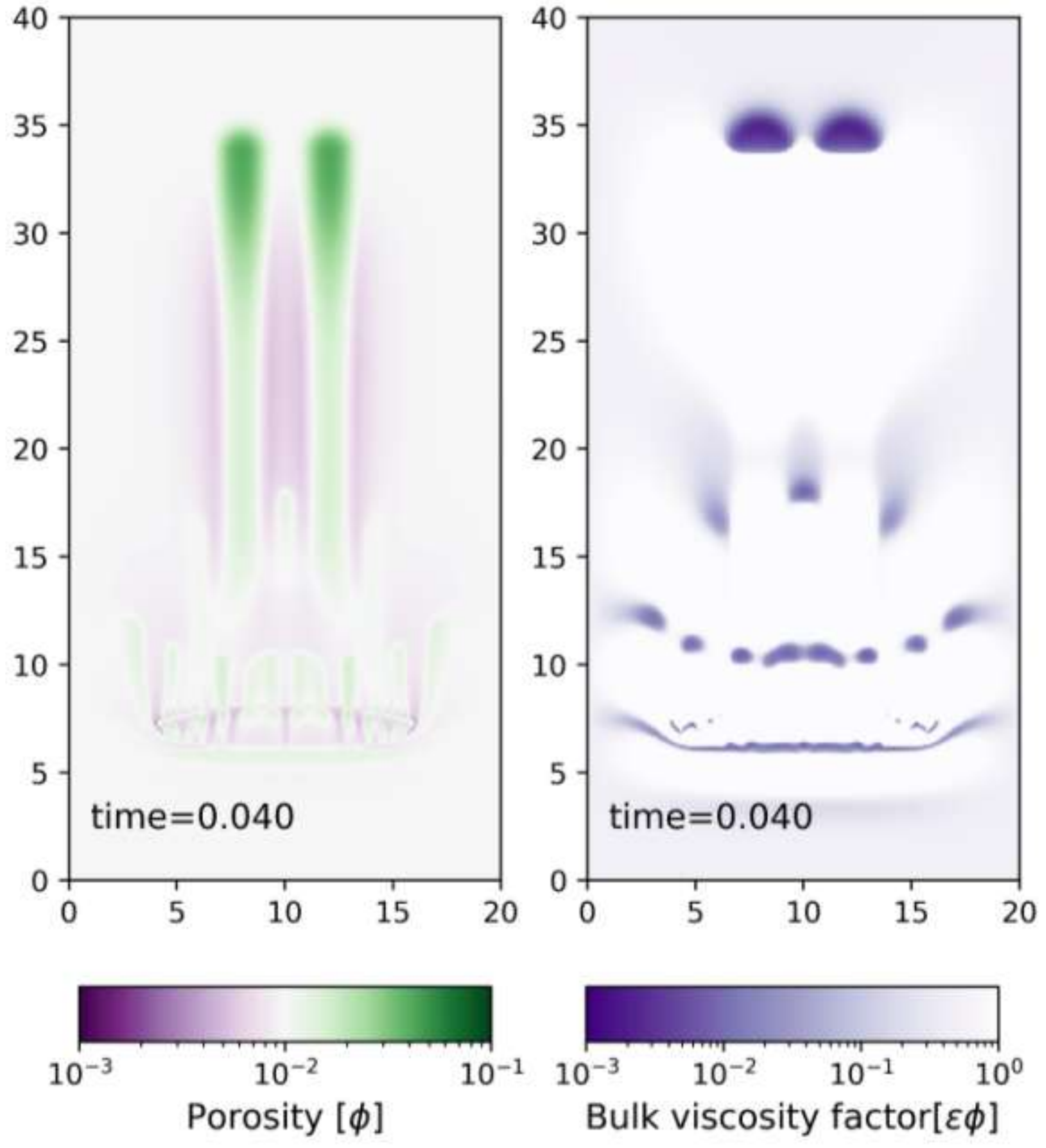

# Result: Type 2 ( $R_v$=10, 30, 100)

## $R_v$= 10

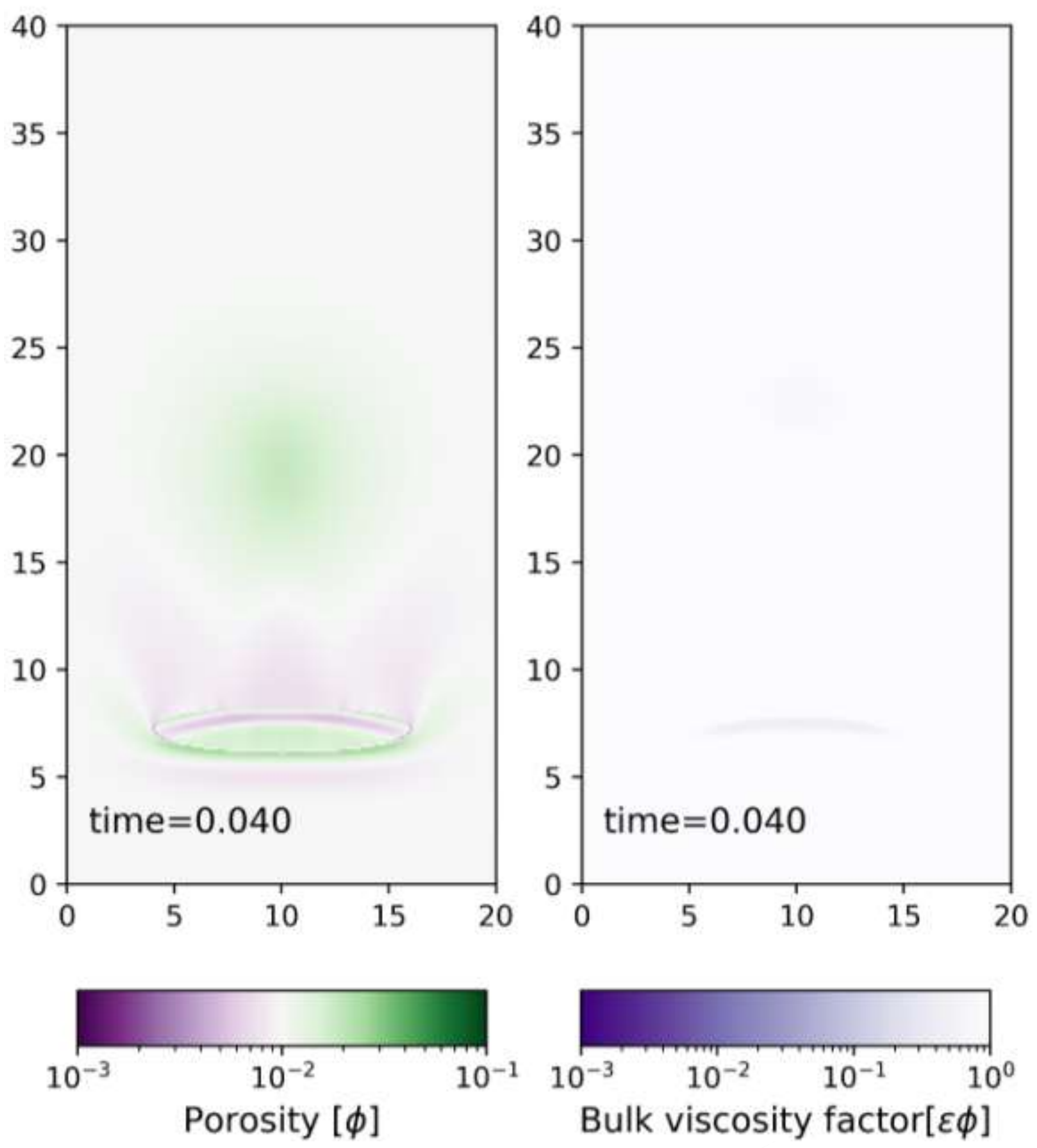


## $R_v$= 30

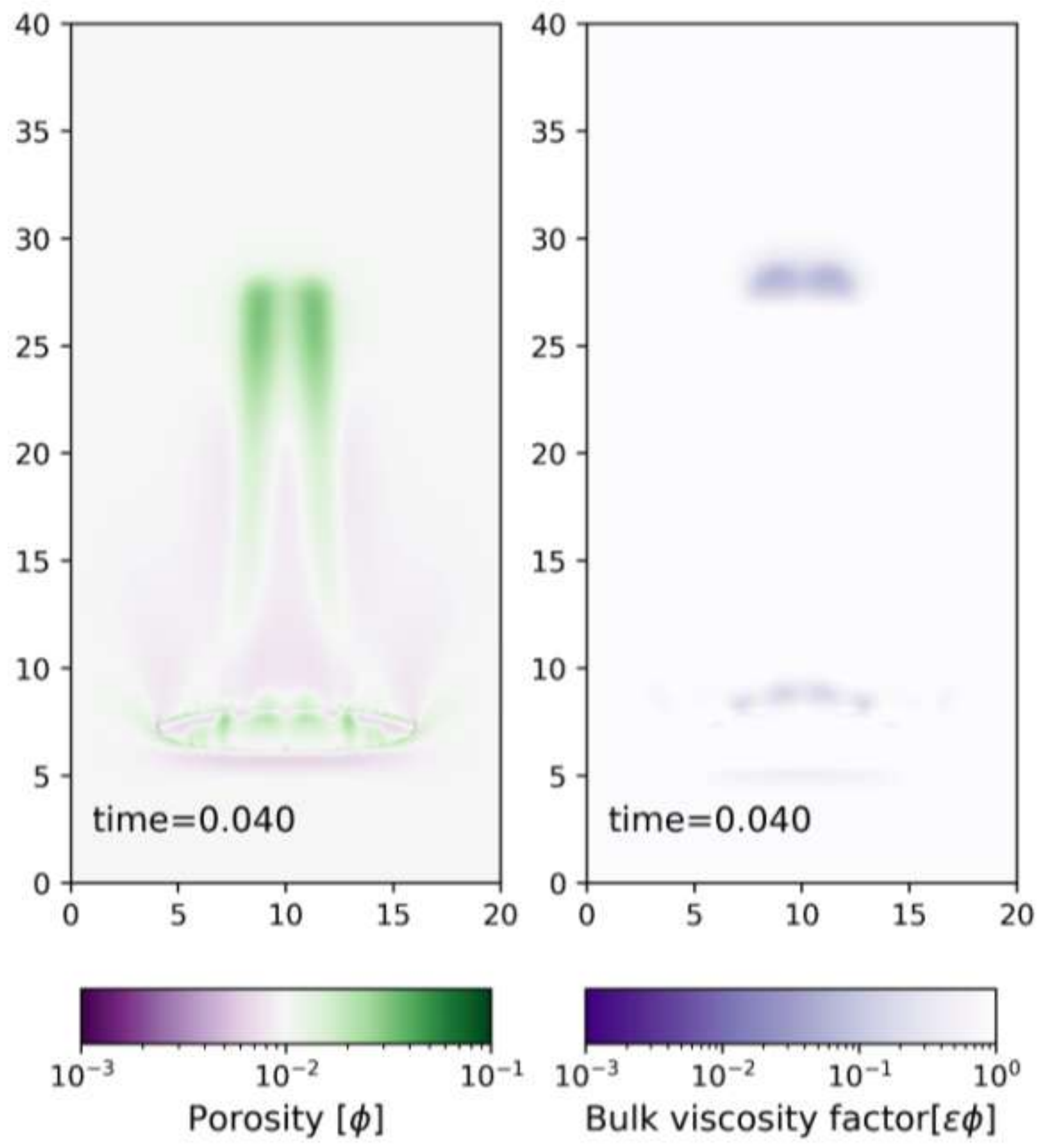


## $R_v$= 100

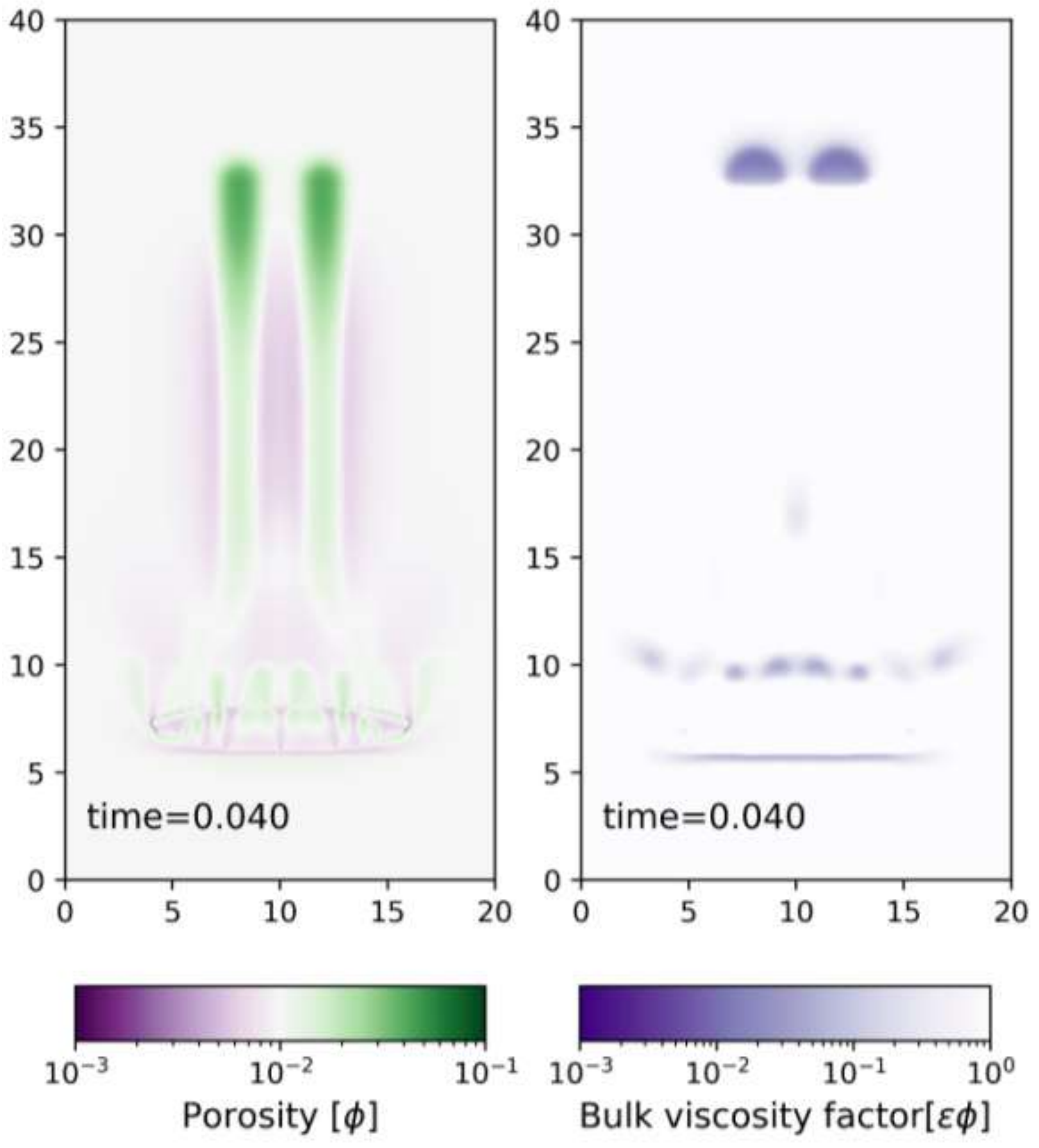

# Result: Type 3 (Rv=20, 30, 100)

**Rv= 20** $\tau_d = \frac{1}{80}$

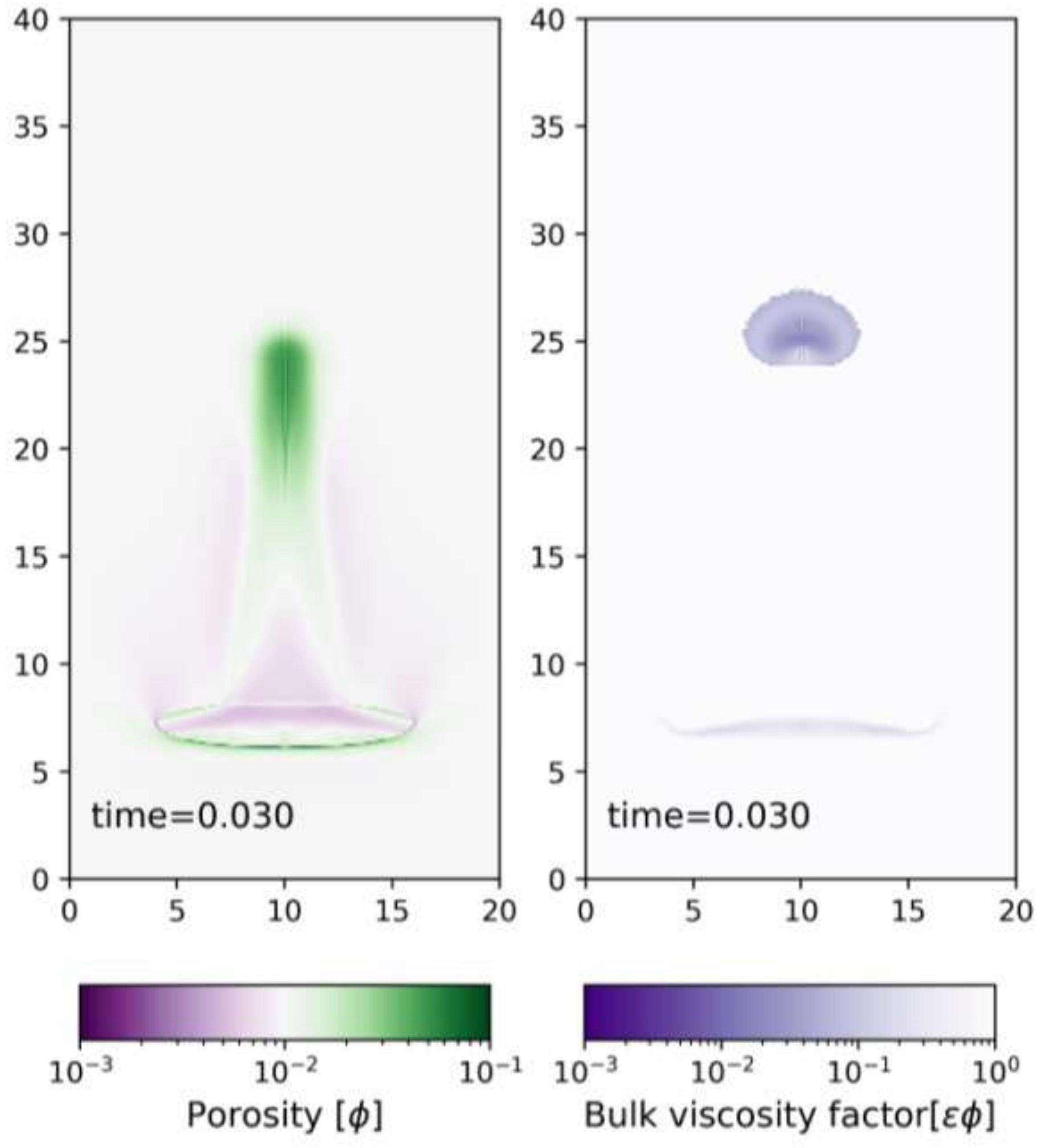


**Rv= 30** $\tau_d = \frac{1}{120}$

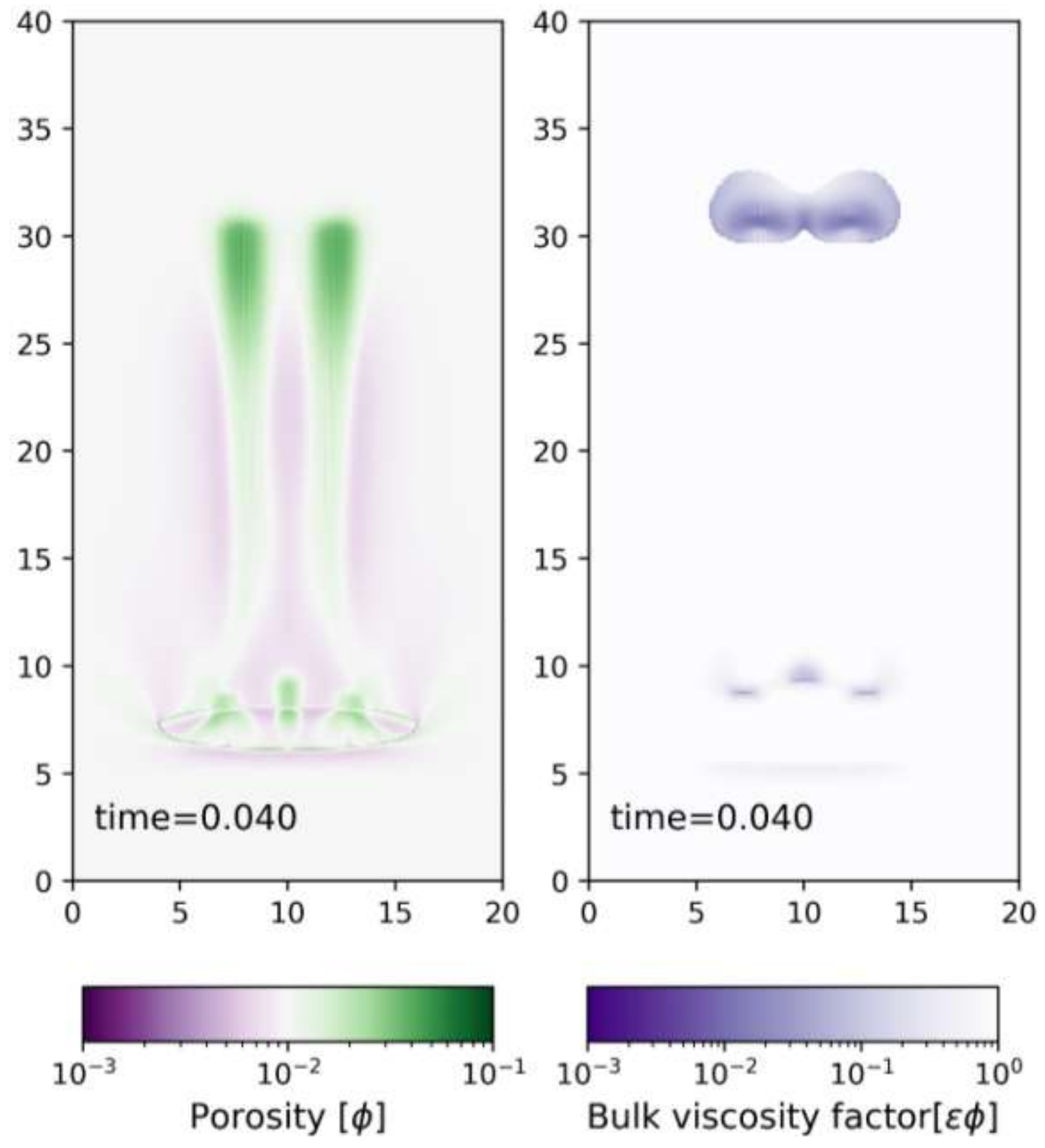


**Rv= 100** $\tau_d = \frac{1}{120}$

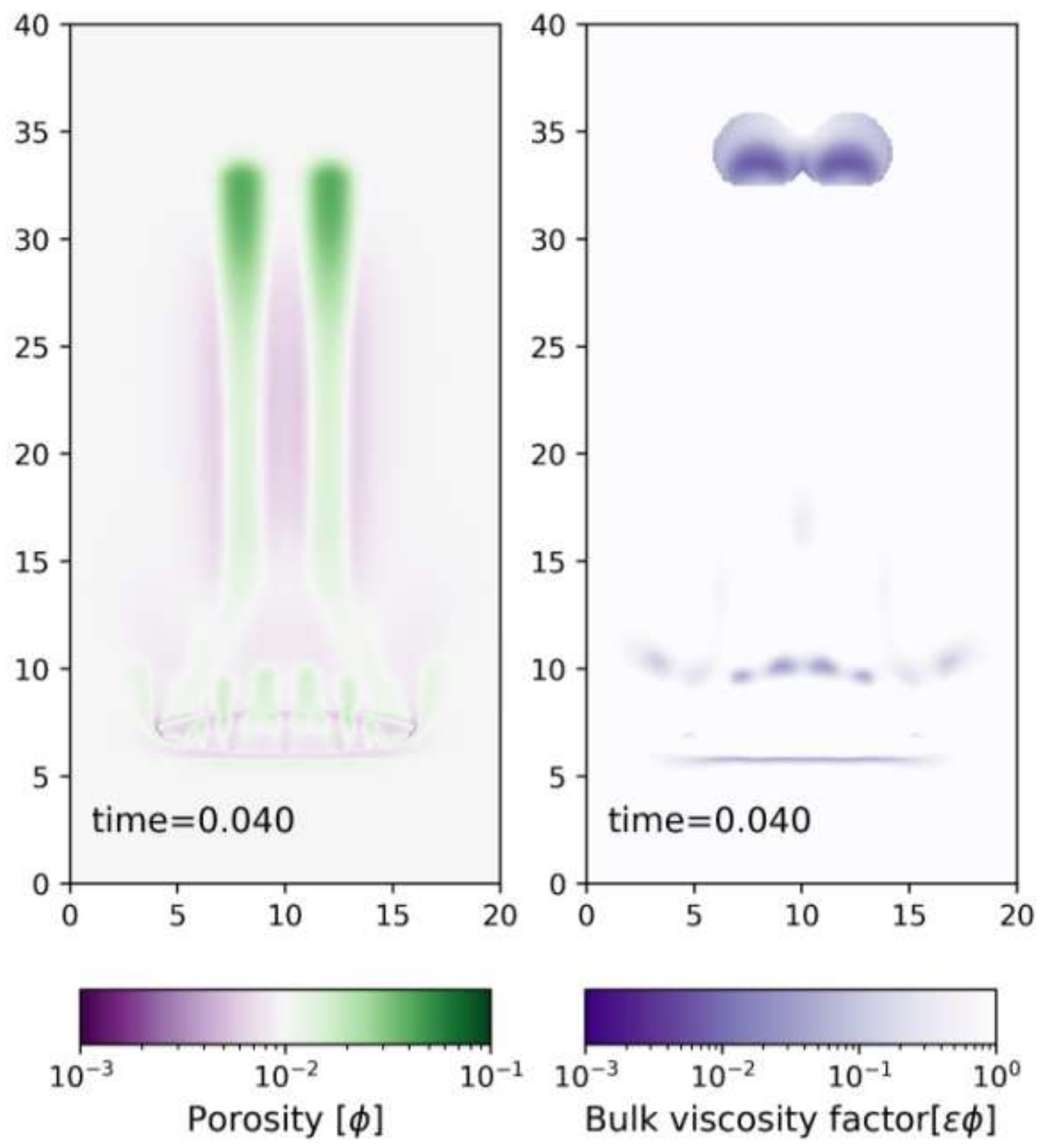

# Results: comparison

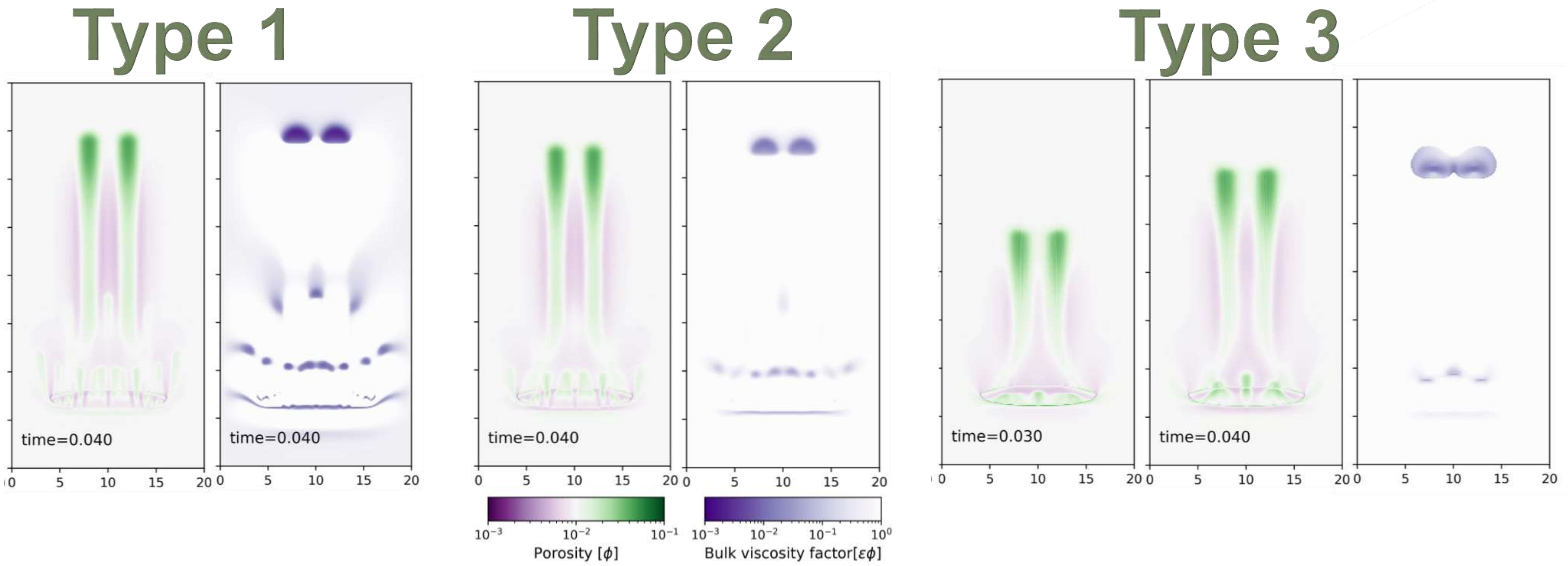


Type 3 rheology with $R_v$=30 produces two channels that has slightly different geometry than Type 1 and 2 models. The wave fronts at the top of the channels are sharper than previous models.  We also observe new and fine porosity structures within the channels.

# Results: comparison

Type 2: $R_v$=30

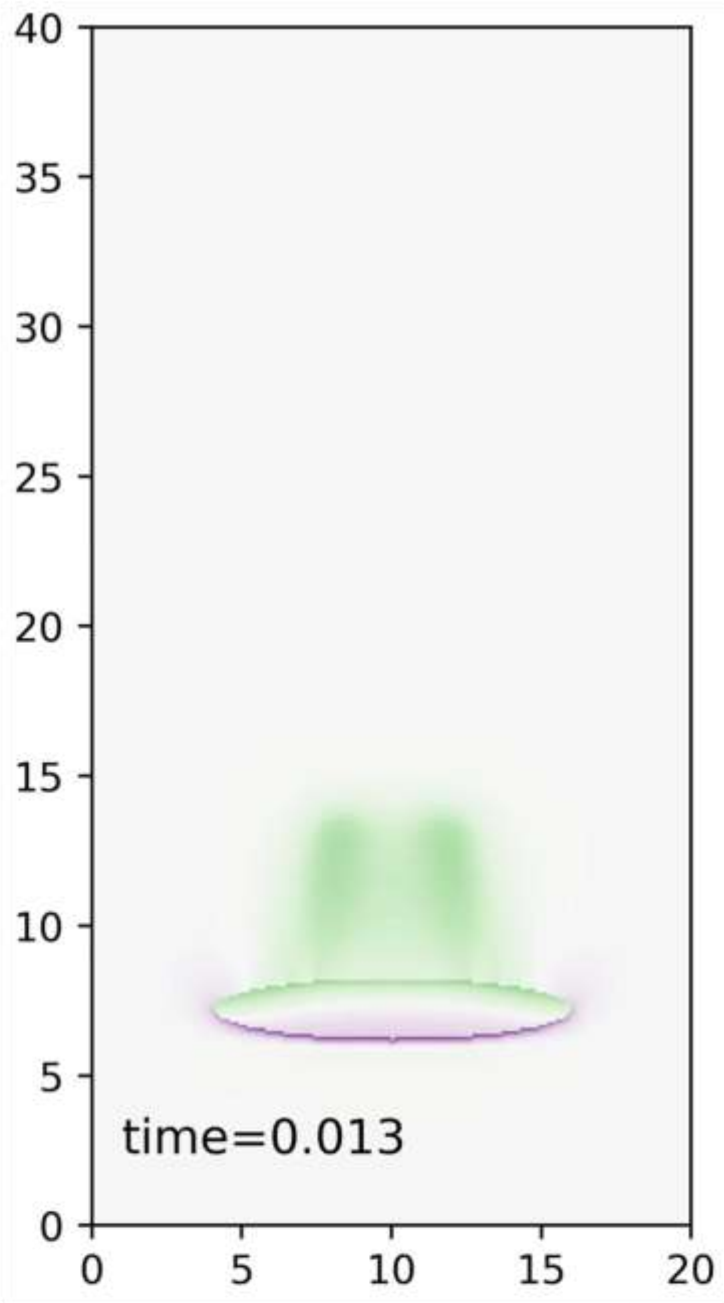


Type 2: $R_v$=30
Weaker $\mu_s$

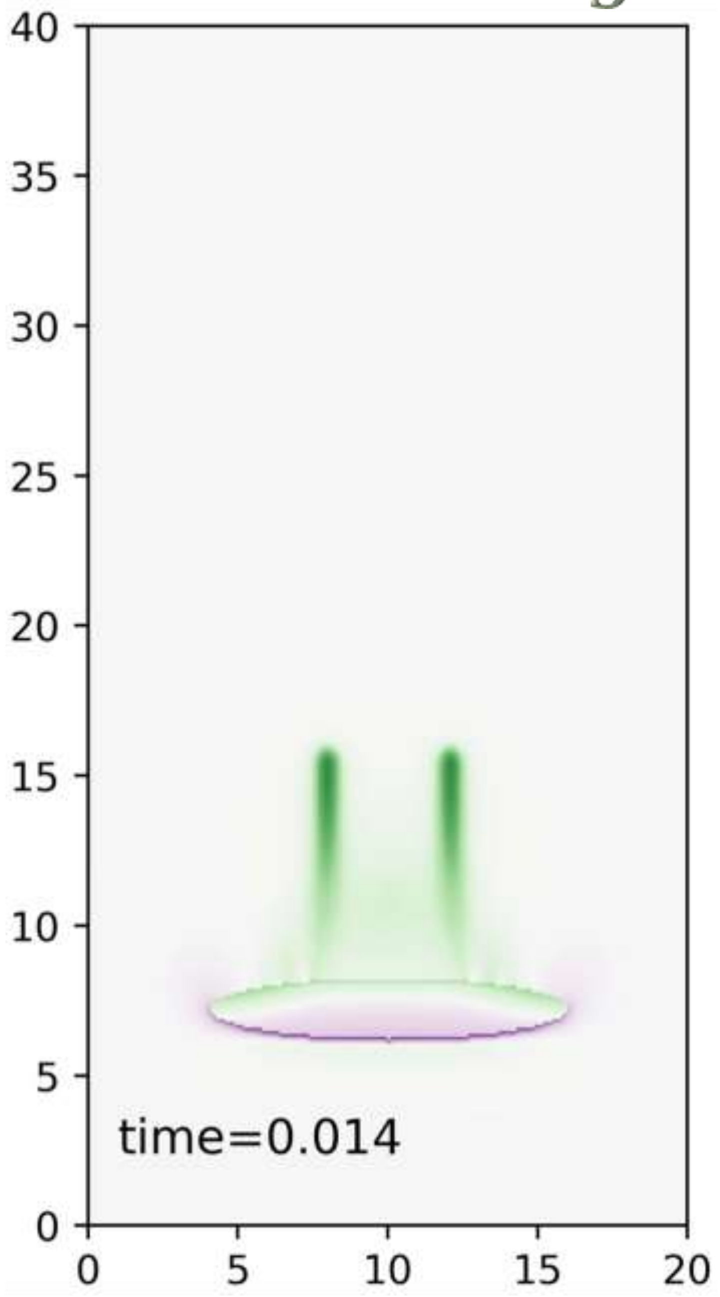


Type 3: $R_v$=30
Weaker $\mu_s$

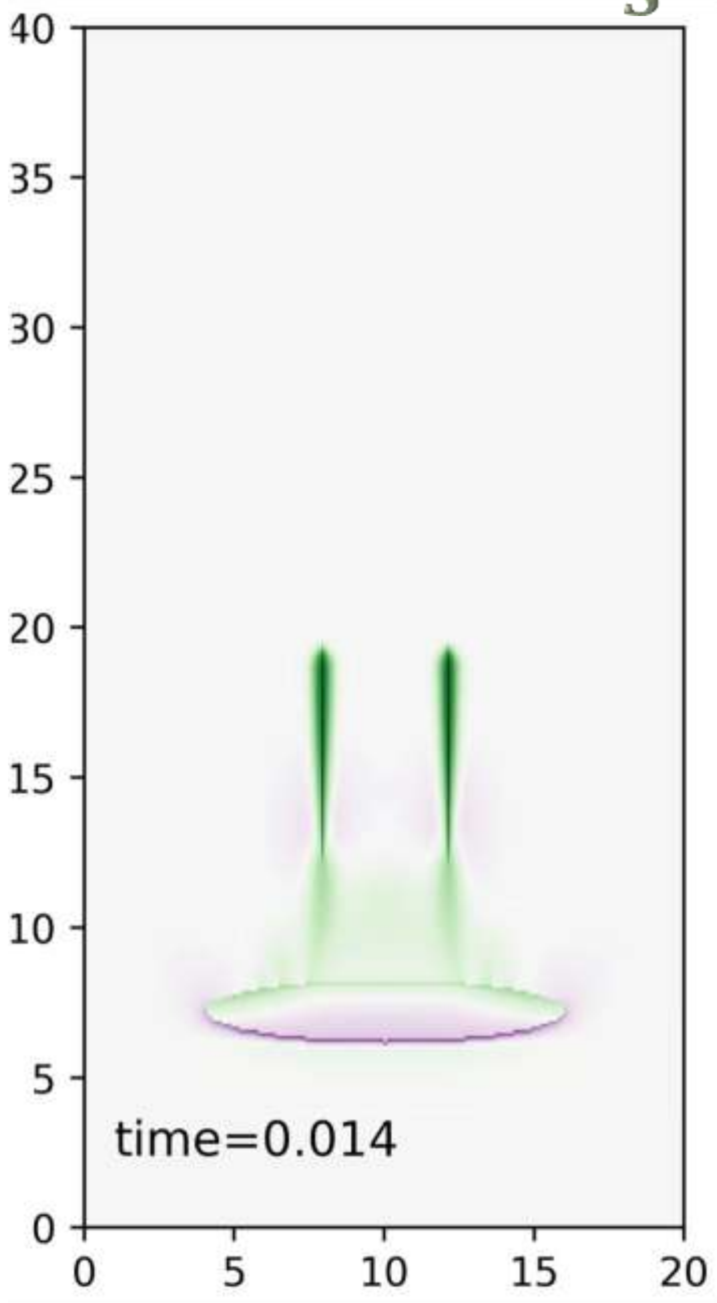


- Our 2D models show that the width of the fluid flow depends on the shear viscosity
- (compare to bulk viscosity) and the shear-enhanced effect may further induce more
- focused fluid flow.

# Scaling to the geological time and space scales

- Length scale: $L_{compaction} = \sqrt{k\frac{\eta_\phi}{\mu_f}} = \sqrt{10^{-20}\frac{10^{14}}{8*10^{-4}}}$

0.035 m for shale

~35 m for sandstone

- Wave velocity scale : $V_{wave} = \frac{\Delta\rho g L_{compaction}^2}{\eta_\phi} = k\frac{\Delta\rho g}{\mu_f} = 10^{-20}\frac{10^4}{8*10^{-4}}$

$\sim 4 * 10^{-6}$ m/year for shale

~4 m/year for sandstone

- Time scale: $\tau_{compaction} = \frac{L_{compaction}}{V_{wave}}$

~8750 year for shale

~8.75 year for sandstone

| | Shale | Sandstone | Units |
|---|---|---|---|
| Bulk viscosity | $10^{11} - 10^{14}$ | $10^{11} - 10^{14}$ | [Pa s] |
| Permeability | $10^{-20}\sim10^{-15}$ | $10^{-14}\sim10^{-13}$ | $[m^2]$ |
| Brine+$CO_2$ viscosity | $8 * 10^{-4}$ | $8 * 10^{-4}$ | [Pa s] |
| Brine+$CO_2$ density | 1020 | 1020 | [kg $m^{-3}$] |

Dong et al 2010
Rass et al. 2014
Rass et a. 2017

# GPU Acceleration

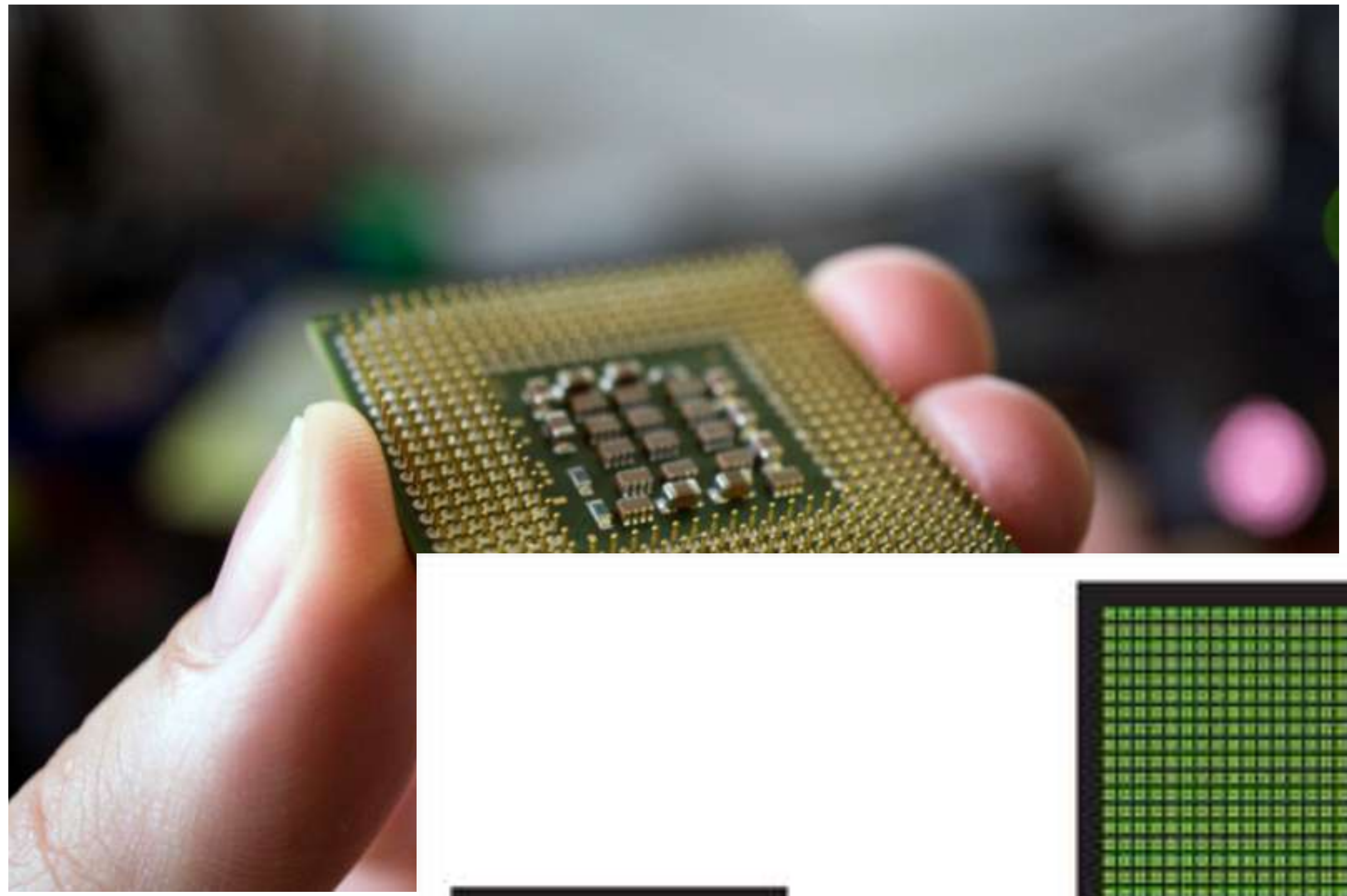


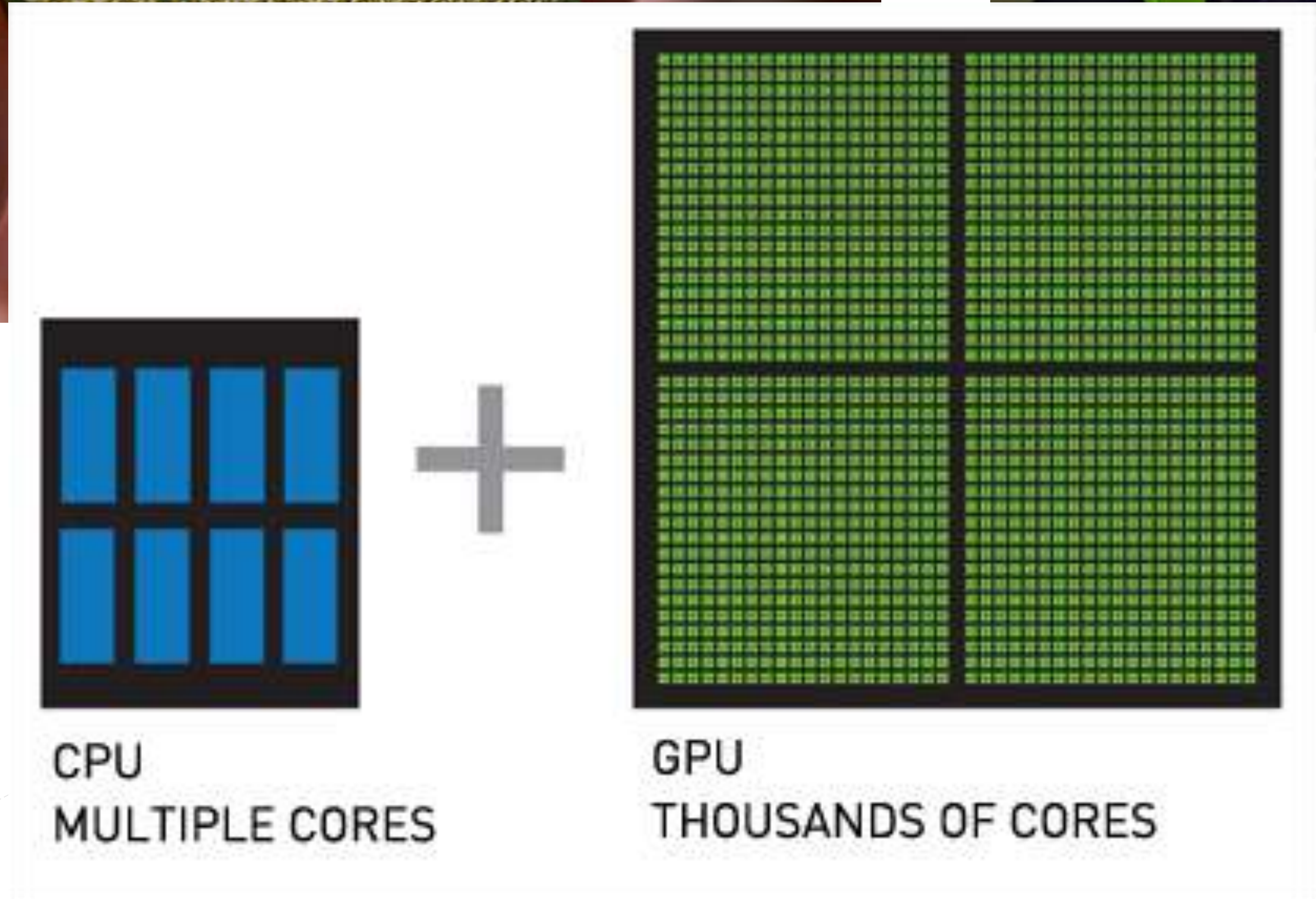


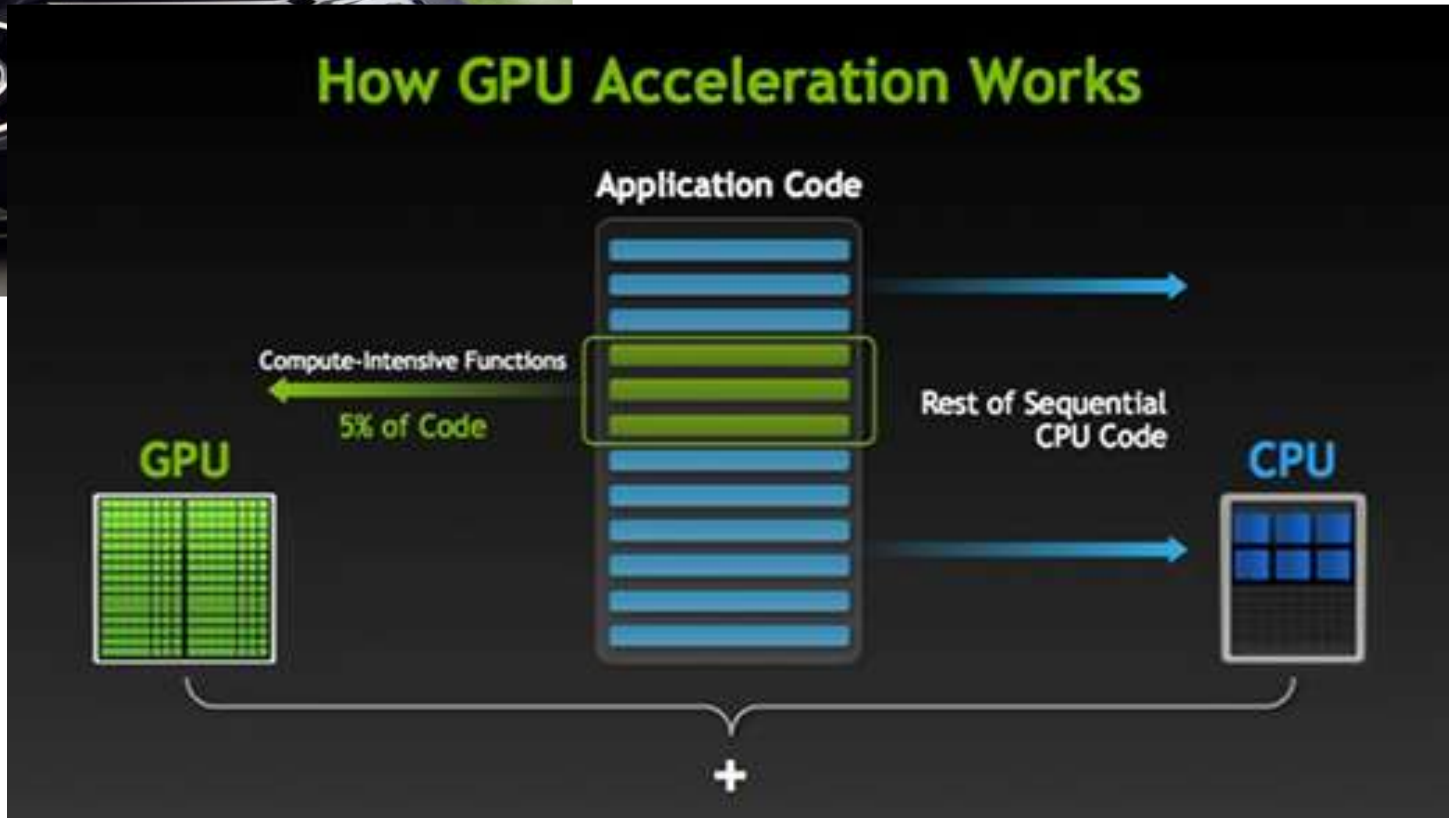

# Numerical method for large-scale modeling

- Finite difference
- Staggered grid
- Pseudo-Transient method
- Dampening scheme
- Multi-device implementation: Matlab + C-cuda

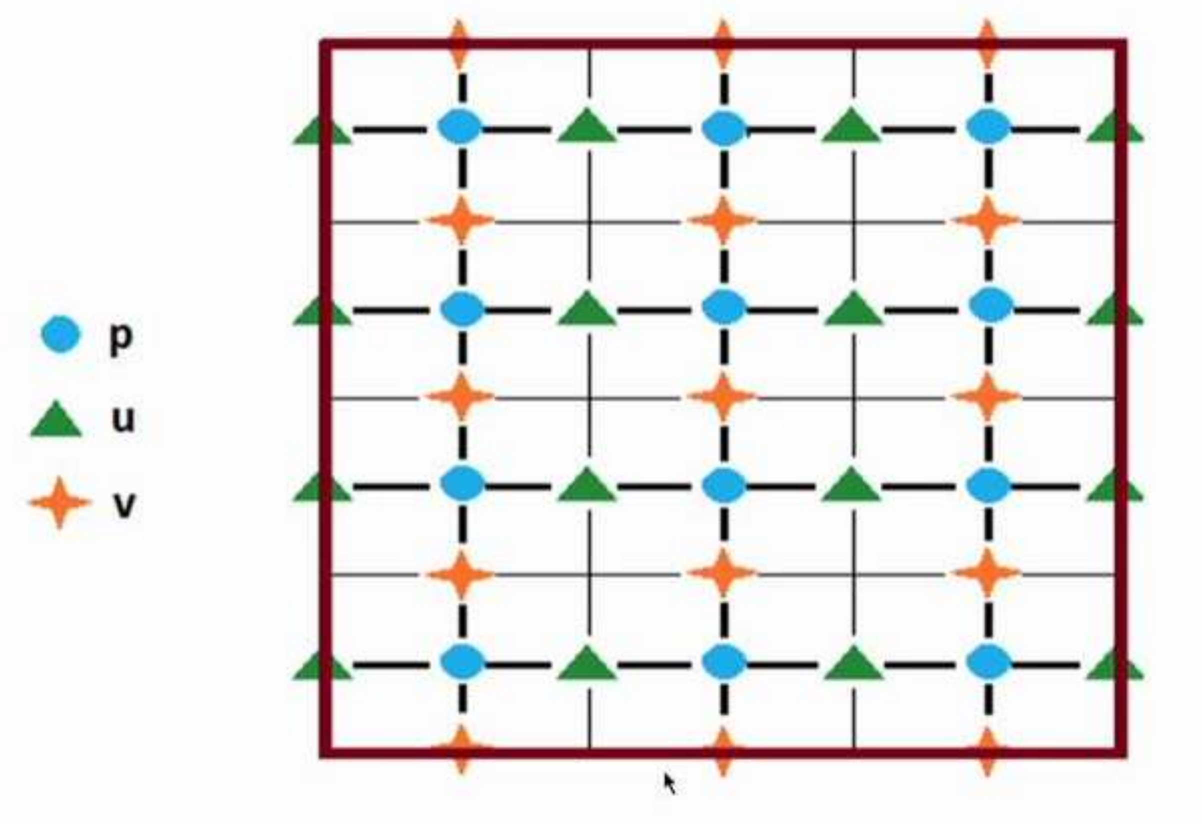


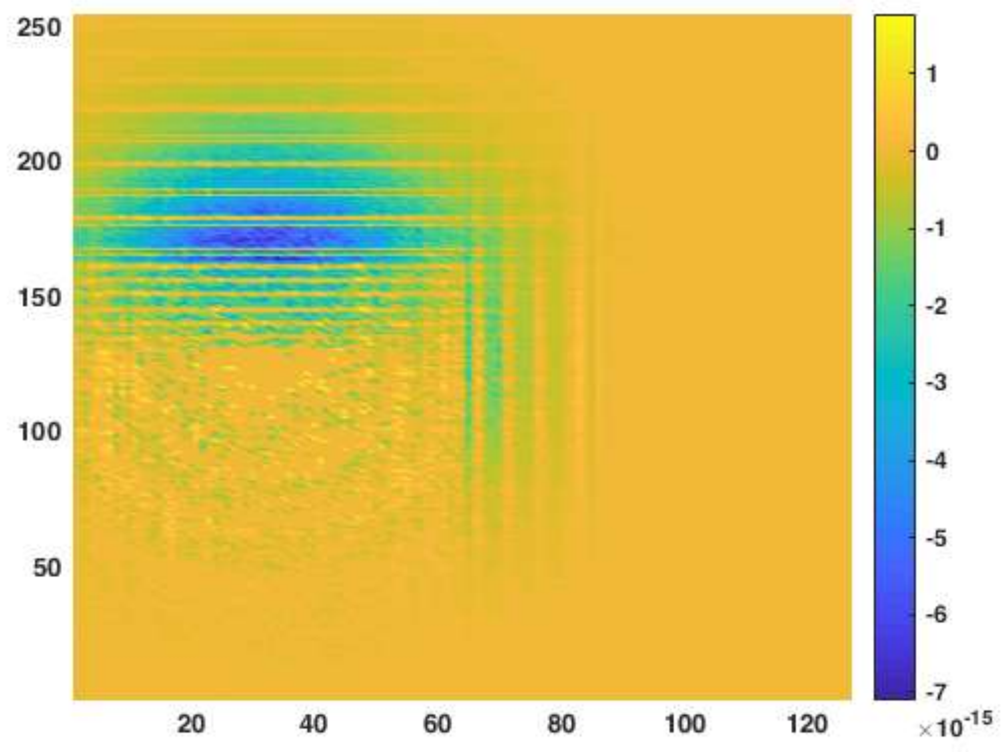


**The scaling of computation complexity**

2D case

Total nodes: N=nx*nx

Iteration times: O (nx)

Computational complexity: O $(\mathrm{n}x^3)$ or $O(N^{\frac{3}{2}})$

3D case

Total nodes: N=nx*nx*nx

Iteration times: O (nx)

Computational complexity: O $(\mathrm{n}x^4)$ or $O(N^{\frac{4}{3}})$

# Conclusion

- Three types of rheology produce quite similar fluid channels under the condition that enough weakening is applied in our models.

- In order to form channelized fluid flow, the tensile strength need to be significantly weaker than the compressive strength.

- The width of the fluid channels are largely depend on the shear viscosity and bulk viscosity,  while the shear-enhanced effects may further localized the fluid flow.

- Pseudo-Transient method with GPU computing provides a promising way of 3D modelling.

# Further work

1. GPU speed up
2. 3D modelling
3. Material layers (reservoir and caprock layers) in the models:
   n (n>2) layer with different material properties ($\phi$,k, $\eta_{\phi}$)
   geological input from seismic data
4. modelling the spreading of fluid underneath the caprock.
5. Elasticity and microseismicity

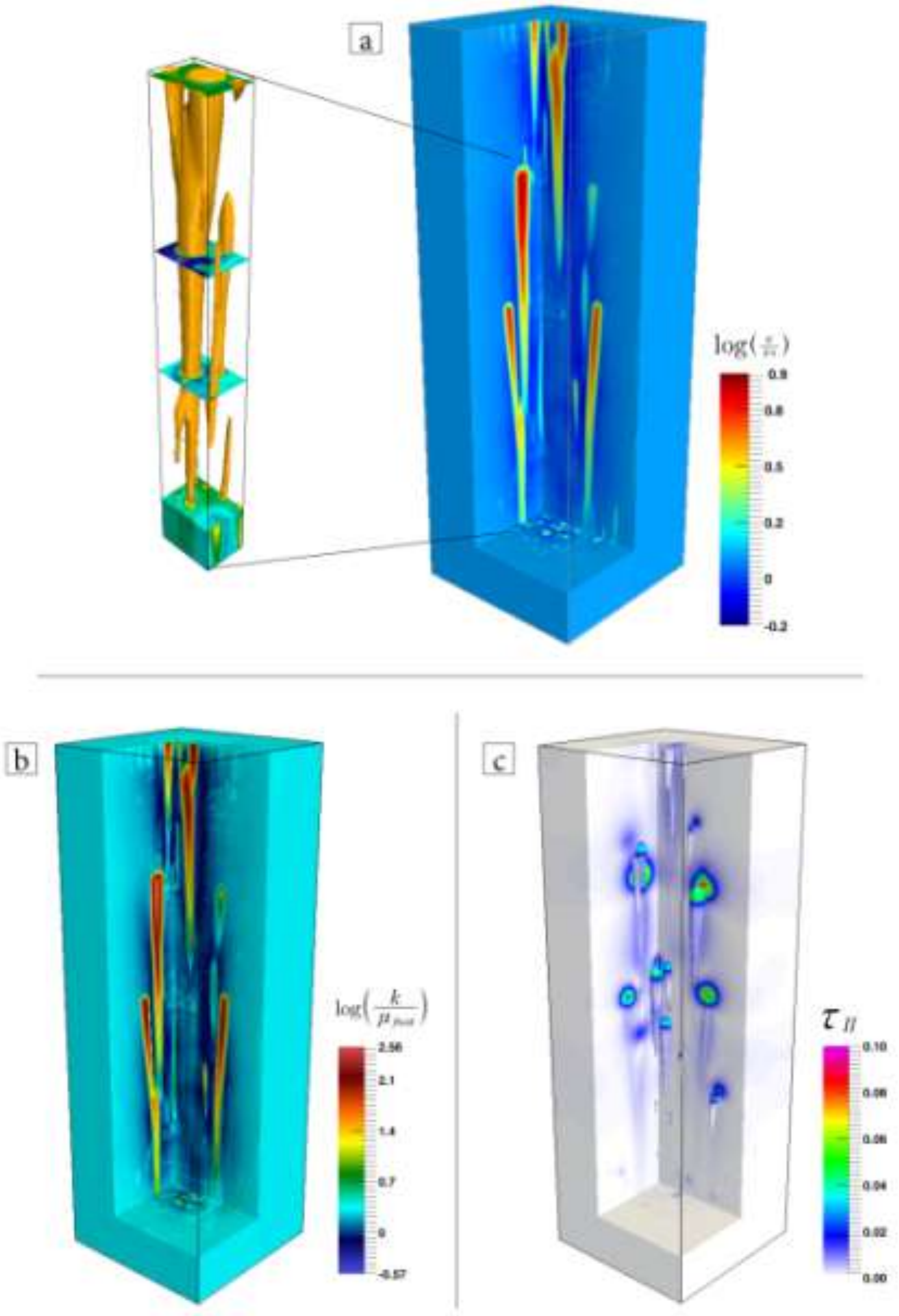

# Scaling to the geological time and space scales

> Length scale

$$L_{compaction} = \sqrt{k\frac{\eta_\varphi}{\mu_f}} = \sqrt{1000 \cdot 2 \cdot 10^{-18}\frac{10^{11}}{8 \cdot 10^{-4}}} \approx 0.5[\mathrm{m}]$$

due to dynamic permeability increase

> Wave velocity scale

$$V_{porosity\ wave} = \frac{\Delta\rho g L^2_{compaction}}{\eta_\varphi} = k\frac{\Delta\rho g}{\mu_f} = 1000 \cdot 2 \cdot 10^{-18}\frac{10^4}{8 \cdot 10^{-4}} \approx 1.0[\mathrm{m/yr}]$$

> Time scale

$$\tau_{compaction} = \frac{L_{compaction}}{V_{porosity\ wave}} \approx 0.5[\mathrm{yr}]$$

| | Nordland Shales | Units |
|---|---|---|
| Effective bulk viscosity | $1 \cdot 10^{11}$ | [Pa s] |
| Permeability | $2 \cdot 10^{-6}$ | [Darcy] |
| Brine + $CO_2$ viscosity | $8 \cdot 10^{-4}$ | [Pa s] |
| Brine + $CO_2$ density | 1020 | [kg m$^{-3}$] |

Values from:
- Dong et al., Mech. Mining Sci., 2010
- Sone and Zoback, Int. J. Rock Mech. Mining Sci., 2014
- Hagin and Zoback, Geophysics, 2004
- Cavanagh, Energy Procedia 37, 2013

See: Räss et al., Energy Procedia 63, 2014 for details

| used symbols | | | |
|---|---|---|---|
| $g$ | gravity | $\mu_f$ | fluid shear viscosity |
| $k$ | fluid permeability | $\eta_\varphi$ | effective bulk viscosity |
| $\mu_s$ | solid shear viscosity | $\Delta\rho$ | $(\rho_s - \rho_f)$ density contrast |

# Result: Type 1 (R=1000,100,10)

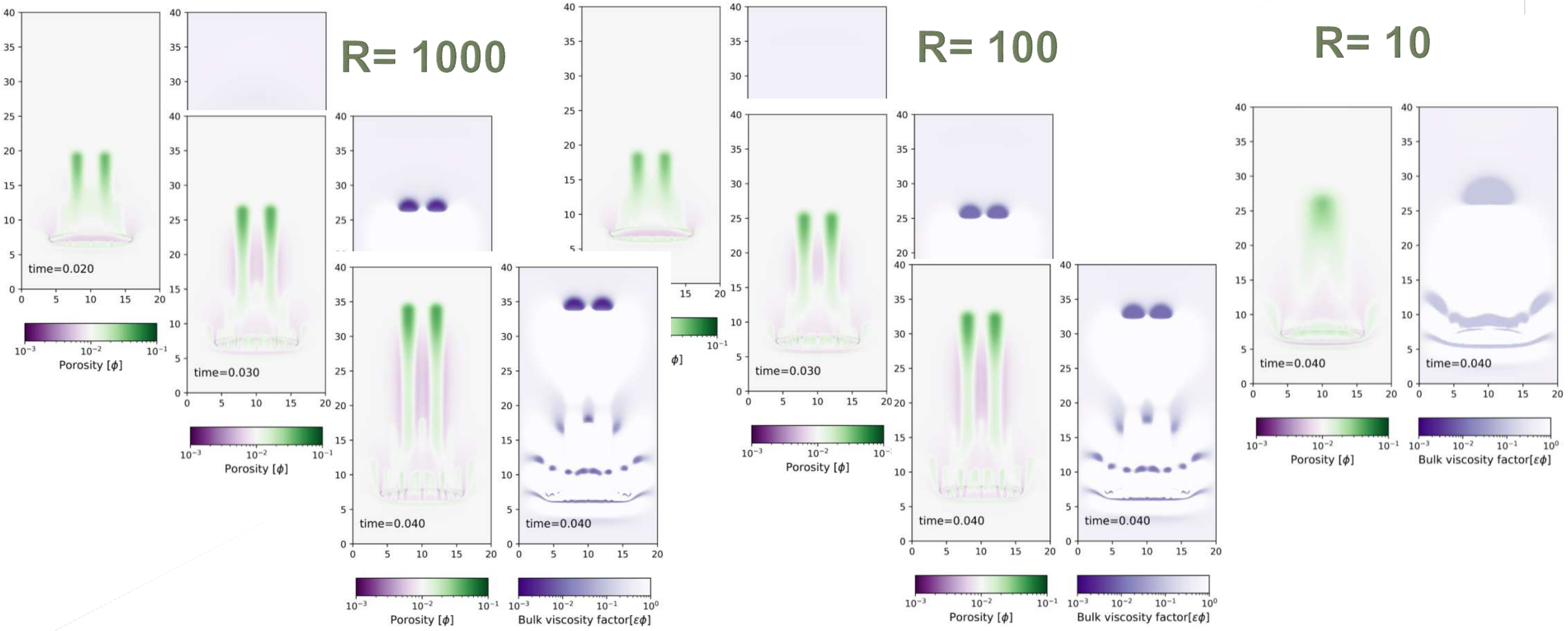

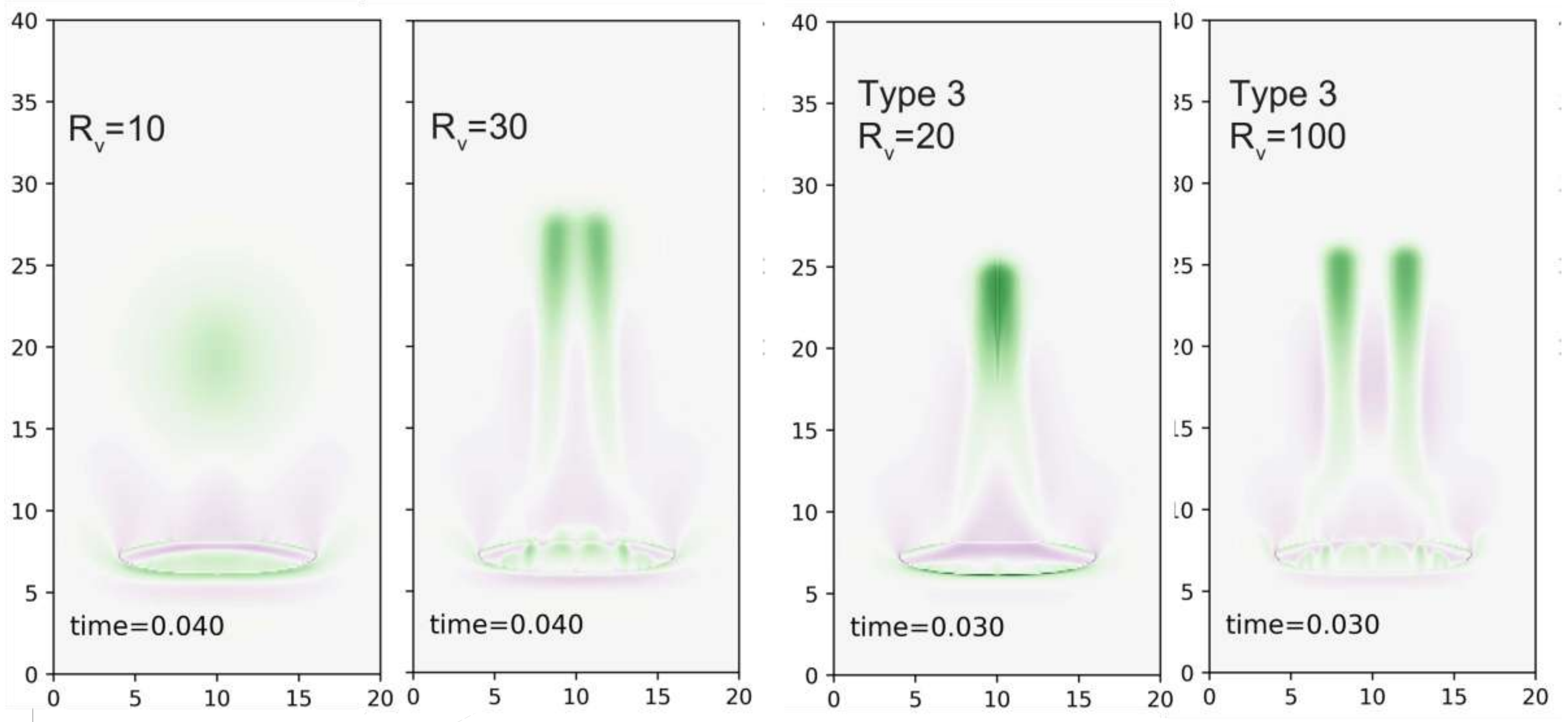


- epsi=$10^{-4}$
- epsi=$10^{-3}$

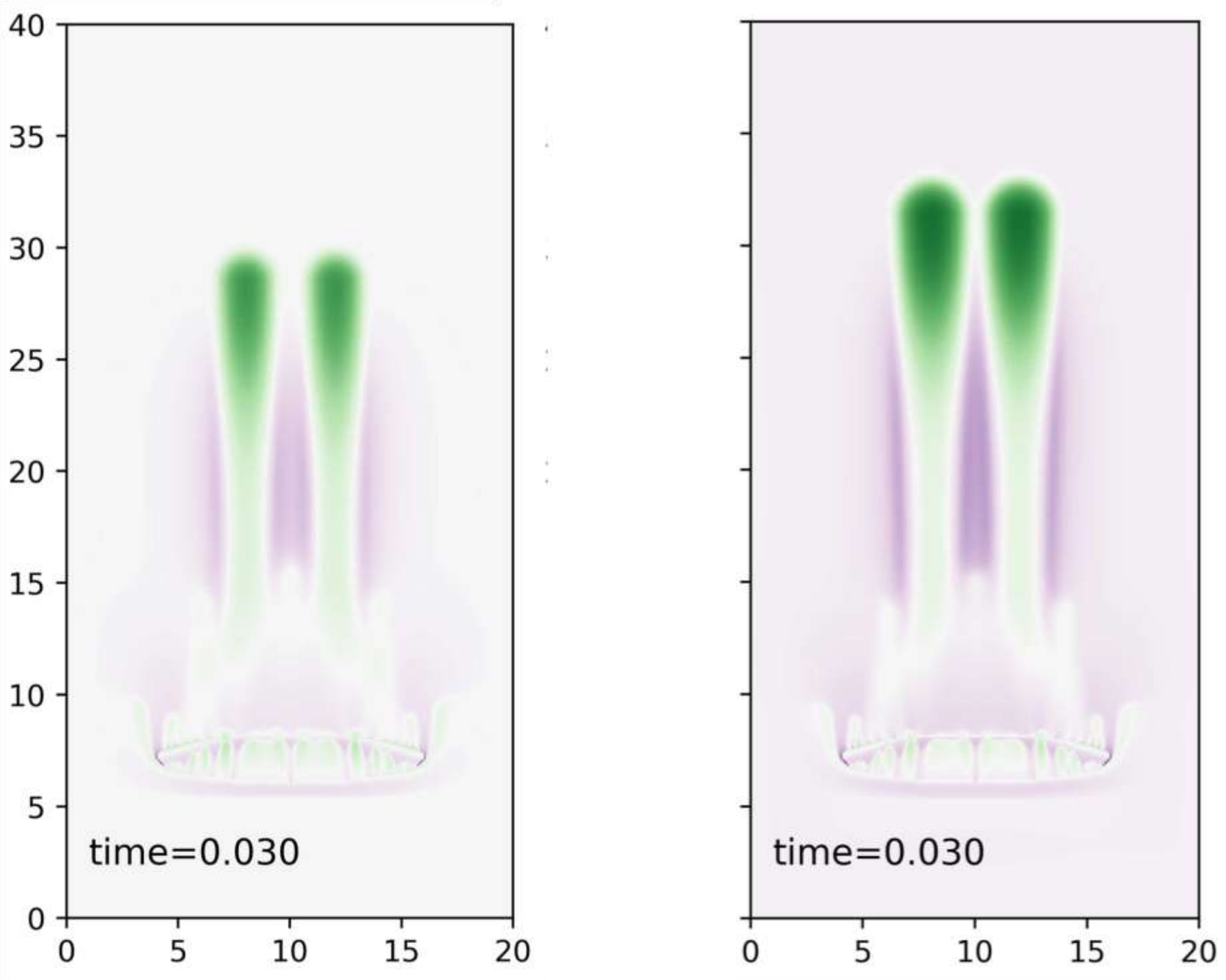

- Fluid flow instability in viscously deforming porous rocks, commonly known as solitary
- porosity waves, has been used to explain formation of seismic chimneys. Experimen
- -tal data show that volumetric deformation of rocks is strongly coupled with shear
- deformation, which leads to shear-induced decompaction at low confining pressure and
- shear-enhanced compaction at higher confining pressure. In this study, we introduce a
- new viscoplastic rheology that takes account on different compressive and tensile
- strengths (different critical pressures for the onset of pore collapse and pore generation)
- and the shear-enhanced weakening of the bulk viscosity. In order to compare with previous
- studies and study the shear-enhanced effects, three types of rheology are used for model
- calculation. The model results shows that our new rheology produces fluid channels
- similar to previous studies that use a simple decompaction weakening factor of R. We
- found that the tensile strength needs to be 30~100 times lower than the compressive
- strength for the formation of focused fluid flow. The shear-enhanced effects introduce
- substantial weakening (i.e. a factor of >100) of bulk viscosity, which reduces the effective
- pressure significantly in the model. Fine porosity structures within the fluid channel are
- observed. This suggests that the shear enhancement of volumetric deformation might be